

Developing a CRISPR-Mediated Knockout TCR Human T Cell Line
for Use in Cloning Antigen-Specific T Cell Receptors

by

Gabrielle Hirneise

A Thesis Presented in Partial Fulfillment
of the Requirements for the Degree
Master of Science

Approved April 2020 by the
Graduate Supervisory Committee:

Karen Anderson, Chair
Douglas Lake
Hugh Mason

ARIZONA STATE UNIVERSITY

May 2020

ABSTRACT

Adoptive transfer of T cells engineered to express synthetic antigen-specific T cell receptors (TCRs) has provocative therapeutic applications for treating cancer. However, expressing these synthetic TCRs in a CD4⁺ T cell line is a challenge. The CD4⁺ Jurkat T cell line expresses endogenous TCRs that compete for space, accessory proteins, and proliferative signaling, and there is the potential for mixed dimer formation between the α and β chains of the endogenous receptor and that of the synthetic cancer-specific TCRs. To prevent hybridization between the receptors and to ensure the binding affinity measured with flow cytometry analysis is between the tetramer and the TCR construct, a CRISPR-Cas9 gene editing pipeline was developed. The guide RNAs (gRNAs) within the complex were designed to target the constant region of the α and β chains, as they are conserved between TCR clonotypes. To minimize further interference and confer cytotoxic capabilities, gRNAs were designed to target the CD4 coreceptor, and the CD8 coreceptor was delivered in a mammalian expression vector. Further, Golden Gate cloning methods were validated in integrating the gRNAs into a CRISPR-compatible mammalian expression vector. These constructs were transfected via electroporation into CD4⁺ Jurkat T cells to create a CD8⁺ knockout TCR Jurkat cell line for broadly applicable uses in T cell immunotherapies.

TABLE OF CONTENTS

	Page
LIST OF TABLES	v
LIST OF FIGURES.....	vi
INTRODUCTION.....	1
Cancer: Modern Medicine’s Greatest Conundrum.....	1
Alternative Modes of Therapy	1
TCR Therapy	2
Downstream Effects of CTL Infusion	3
The T Cell Type	4
Pairing α and β Chains	5
Experimental Design for Cloning Functional TCRs	6
The Hybridization Problem	7
Gene Editing Technology	9
How CRISPR Came About	10
How CRISPR Works	11
Downsides of CRISPR	12
Experimental Design.....	13
METHODS	14
Antigen-Specific T Cell Expansion	14
Sequencing FluM1-Specific T Cell Receptors	14
Designing Primers with Site-Specific Attachment Sites.....	1

METHODS	Page
Gateway Reaction	15
Transfection of FluM1-Specific TCRs	16
Tetramer Staining and Flow Cytometry Analysis	16
Guide RNA Design	18
Phosphorylation of Oligos	18
Annealing Oligos	19
Cultivating PX458 Vector.....	19
Golden Gate Reaction	19
Transfection of PX458 Construct	20
Antibody Staining and Flow Cytometry Analysis.....	20
MGH CRISPR Sequencing	21
RESULTS.....	23
Cloning FluM1-Specific T Cell Receptors	23
Flow Cytometry Analysis of KSA FluM1 Clone	24
Annotated Jurkat TCR Sequences	25
Guide RNA Design for α Chain	26
Guide RNA Design for β Chain	28
Confirmation of Double-Stranded Synthesis of Guide RNAs	30
Confirming Integration of Guide RNAs into PX458	31
Validation of Guide RNAs in PX458	32
DISCUSSION	33
Solving Cancer Through a Modern, Alternative Approach	33

DISCUSSION	Page
Adoptive Cell Transfer.....	33
Competing Receptors in TCR therapy.....	35
TCR KSA Clone Transfection Characterization	37
How to Combat Hybridization.....	37
Guide RNAs and Off-Target Potential	38
Why Golden Gate Cloning.....	38
Why the PX458 Vector	40
What is the Best RNP Delivery Method.....	41
What Makes CRISPR the Best Gene Editing Protocol	42
Gene Editing Accuracy	43
Developing a Functional CD8+ T Cell Line	44
REFERENCES	46
APPENDIX	56
A SUPPLEMENTARY TABLES	56
1. Guide RNA Designs for α Region of the Jurkat TCR Sequence.	57
2. Guide RNA Designs for β Region of the Jurkat TCR Sequence.	57
3. Reverse Primer Design for Guide RNA Amplification and Sequencing	58
4. One-Step PCR Protocol for Amplification of Guide RNAs	58

LIST OF TABLES

Table		Page
1.	Selected Guide RNA Designs for the α Constant Region.....	27
2.	Selected Guide RNA Designs for the β Constant Region.....	29

LIST OF FIGURES

Figure		Page
1.	Annotated Sanger Sequencing Results for the TCR α Sequence.....	23
2.	Annotated Sanger Sequencing Results for the TCR β Sequence.....	24
3.	Flow Cytometry Analysis of TCR Construct in NonA2 PBMCs.....	24
4.	Flow Cytometry Analysis of TCR Construct (Negative Control)	25
5.	Validated Jurkat TCR Sequence for α and β Chains	26
6.	On-Target and Off-Target Values for α Chain Guide RNA Designs	27
7.	Location and Orientation of α Chain Guide RNAs	28
8.	On-Target and Off-Target Values for the β Chain Guide RNA Designs	29
9.	Location and Orientation of the β Chain Guide RNAs	30
10.	Annealed Guide RNA Oligos Relative to the Sense Strand	30
11.	Amplification of α and β Guide RNA Inserts in the PX458 Vector	31
12.	Annotated Sequencing Results for PX458 and the Guide RNA Inserts	32

INTRODUCTION:

Cancer: Modern Medicine's Greatest Conundrum

Cancer, one of modern medicine's most cumbersome conundrums, is the second leading cause of death worldwide [1]. Due to a variety of subtypes and the rapid evolution of cancer cells, there is no one-size-fits-all strategy to vanquish cancer in its entirety. Establishing one course of treatment is made especially hard due to there being at least six hallmarks of cancer cells [2]. In recent years, two additional hallmarks have emerged, one being the evasion of immune destruction [2]. Not only does targeting just one prove to be insufficient for long-term survival and the prevention of treatment resistance, but there is also the concern that cancer cells evolve the ability to evade the host's immune system [3]. Mediating this hallmark by bolstering this immune response could spell success for cancer treatment. Unfortunately, current standard-of-care practices include chemotherapy and radiation, which for hard-to-treat subtypes or for late-stage cancers that have metastasized, don't work or serve only as a short-term fix, leading researchers to seek other forms of therapy [4].

Alternative Modes of Therapy

Alternative therapies currently being explored include cancer vaccines, checkpoint inhibitors, immunoglobulin supplementation, and methods for adjusting the tumor microenvironment [5]. Amongst some of the more appealing modes of treatment is adoptive cell transfer, where immune cells are extracted and amplified for re-infusion, or cell lines are engineered to target cancer cells and promote cell-killing capabilities [6]. These alternative therapies are intended to reduce the toxicity conferred by

standard-of-care treatments while bolstering one's immune response, and they can be utilized as part of combination therapies or in forms of adaptive therapy.

TCR Therapy

Adoptive T cell transfer, a provocative immunotherapy, is being widely pursued for its specificity and programmability. Amongst adoptive T cell therapy, there is tumor-infiltrating (TIL) therapy, where pre-existing cytotoxic T cells specific to tumor antigens are activated and amplified before re-infusion, engineered T cell receptor (TCR) therapy, where T cell lines are engineered to express antigen-specific TCRs that will guide immune cells to the tumor site and induce cell killing, chimeric antigen receptor T cell (CAR T) therapy, where synthetic receptors are assembled at the cell surface to recognize cancer antigens aren't presented via an MHC molecule, and natural killer (NK) cell therapy, which employs the aforementioned strategies but with NK T cells as opposed to CD8+ cytotoxic T cells [7–10]. Though CAR T therapy is an advantageous mode of therapy for targeting cancer cells evading immune recognition, and though TIL therapy involves fewer steps, engineered TCR therapy allows researchers to overcome the ever-evolving nature of cancer epitopes, preventing treatment resistance and enabling clinicians to customize the therapy to the stage and nature of patients' cancer subtype. Additionally, pre-existing clinical trials have proven more effective against solid tumors for TCR therapy as opposed to CAR T therapy, which has been primarily catered towards bloodborne cancers such as lymphoma [11].

Downstream Effects of CTL Infusion

Because the innate and adaptive arms of the immune system inform each other, boosting T cell response has downstream effects beyond amplified cell killing. CD8+ killer T cells, upon activation, release cytokines to recruit other immune cells or mediate an inflammatory response to infection [12]. For example, CTLs modulate the release of IFN- γ , TNF- α , and TNF- β to either promote a pro-inflammatory or anti-inflammatory response or to indirectly mediate cell killing [13]. However, this could also pose a problem if the infusion of CTLs initiates a hyperinflammatory environment where DNA damage and tissue degradation ensue [14]. Researchers and clinicians design T cell therapies with this in mind. Maintaining the healthy distribution of activated immune cells between the innate and adaptive arm is critical to developing effective modes of cancer killing that don't put patients at risk of other inflammation-related ailments.

T Cell Diversity

Immunology is a burgeoning field with several unanswered questions, leaving researchers with a high degree of uncertainty in developing immunotherapies. For example, it is hard to project the correct course of action in designing TCRs due to a highly diverse T cell repertoire. It is estimated that there are $10^{13} - 10^{16}$ TCR clonotypes, but there are only 4×10^{11} T cells circulating the human body [15,16]. Beyond projections, the current extent of TCR diversity is unknown, but it is understood that the process of somatic recombination accounts for this high level of diversity [17]. During somatic recombination, the antigen-recognition site of the T cell receptor is formed, creating three loops (CDR1, CDR2, and CDR3). The CDR3 region is comprised

of recombined V(D)J gene segments and makes contact with the peptide presented by MHC molecules, while the CDR1 and CDR2 loops make contact with the MHC molecules themselves [18,19]. For this reason, the CDR3 region is of more relevance to the antigen-presenting cell and accounts for most of the diversity we see in TCRs [18,19]. This variability is responsible for many of the problems that arise in implementing TCR therapy, where researchers have to determine which TCR will target which antigens and whether the peptide being presented on the cell surface is immunogenic. Of great clinical concern is the potential for mistaking foreign antigens for self-antigens, leading to harmful and oftentimes lethal forms of autoimmunity [20].

The T Cell Type

TCRs are heterodimers composed of either $\alpha\beta$ chains or $\gamma\delta$ chains, both made up of variable regions (V) and constant regions (C) anchored to the membrane by a transmembrane protein [21]. $\gamma\delta$ T cells, which are structurally similar to $\alpha\beta$ TCRs, are typically confined to the gut mucosa and are far less common, making up only 0.5–5% of T cells [22]. For that reason, $\alpha\beta$ TCRs are of more clinical significance in T cell-mediated immunotherapies, although $\gamma\delta$ T cells are being explored as candidates for T cell therapies in light of the fact they are MHC-unrestricted and recognize a variety of cellular signals [23]. Among types of T cells, there are CD4⁺ helper T cells, CD8⁺ cytotoxic T cells, regulatory T cells, and natural killer T cells [24]. CD8⁺ T cells use the CD8 co-receptor to bind to the antigen-presenting cell and trigger the release of cytotoxic molecules perforin and granzyme to kill infected or cancerous cells, while CD4⁺ T cells use the CD4 coreceptor to bind to the APC and release cytokines that either signal for the

activation of cytotoxic T cells, B cells, or innate immune cells (macrophages and neutrophils) [25,26]. All T cell types are being explored as potential cancer neutralizers, but it's CD8+ T cells that are responsible for direct cell killing, making them the primary focus in adoptive cell transfer.

Among T cell types, there are naïve and memory T cells – naïve T cells respond to antigens never encountered by the immune system while memory T cells recognize previously encountered antigens and amount a quicker and more effective immune response [27]. These memory T cells represent a high proportion of the T cell population but a low proportion of T cell variability, and the TCRs existing on naïve T cells have high variability but are not expressed in high quantities [28]. At the peak of immune response, antigen-specific T cells can make up about 25 percent of the lymphocyte population, a proportion that was only recently considered to be so high [28].

Pairing α and β T Cell Chains

The TCR heterodimer is composed of the α and β chain, each with their own distinct sequence [29]. Pairing these chains to produce a functional TCR is a prominent challenge in effective cloning and expression – mispairing these separate entities prevents any level of functionality from the T cell [30]. To overcome this challenge, researchers have devised both bulk and single-cell sequencing methods. One popular bulk method is the multiplex primer approach, in which a cDNA sample is tested with a mix of known variable region primers and constant or joining region primers; however, this is limited to known TCR sequences [31]. Other bulk methods apply algorithms to bulk sequencing data to pair α and β chains based on their frequency in a given population [31].

Single-cell methods utilize cell-based emulsion methods to isolate single T cells in oil emulsion droplets, in which the α and β chains from a single cell are fused via reverse transcription [31]. Single cell methods fuse the sequences upstream of cloning, but such methods are costly. Potential mispairing of the chains would render TCR therapy unsuccessful or could produce hybridized TCRs targeting the wrong antigens and potentially killing healthy cells.

Experimental Design for Cloning Functional TCRs

To develop a pipeline for the construction and expression of antigen-specific TCRs, a variety of stimulation methods, cloning protocols, and characterization strategies were explored. First, as a proof-of-concept experiment, T cells were stimulated with the FluM1 peptide. Upon bulk sorting and T cell expansion, RNA was extracted and converted to cDNA by reverse transcription. Using a multiplex PCR approach, the TCR sequences were isolated and amplified. On the VDJdb database, in high frequency, TCR α variable region 17-01, TRAC, TCR β variable region 19-01, and TRBC were observed. Upon amplifying these sequences from the cDNA samples, the α and β chains were cloned into expression vectors separately. Gateway cloning and Golden Gate cloning were both entertained as options in lieu of traditional restriction enzyme cloning. Gateway cloning was more thoroughly explored due to the fact that it utilizes att sites, which contain mutations that eliminate stop codons and ensure that the correct orientation is maintained throughout the cloning process [32]. In the BP reaction, the amplified PCR products were inserted into a pDONR vector via recombination at the att sites, and in the subsequent LR reaction, the pENTR vector was recombined with pcDNA3.2

(a mammalian expression vector) to form the expression clone containing the original insert. Via electroporation, the expression clone was transfected into HEK293 cells, a human kidney derivative, and Jurkats, an immortalized CD4+ human T cell line [33,34]. Tetramer staining and subsequent flow cytometry analysis was performed on the final product; however, conclusions could not be drawn from the results. Because HEK293 cells do not possess the internal machinery of a T cell, which includes the signals for cytokine release, the mechanics for proliferative signaling, and the accessory proteins needed for assembly and activation at the membrane, Jurkats were the optimal candidates for downstream clinical applications. Though HEK293 cells could be utilized to confirm whether TCRs can assemble at the membrane, there is no way to test functionality or T cell activation. Jurkat cells, on the other hand, posed a different problem.

The Hybridization Problem

The results of transfection in Jurkat cells were inconclusive. This is due, in part, to the fact that cloning synthetic TCRs into cell lines possessing endogenous TCRs results in competition between the receptors for accessory proteins such as CD3 and stimulatory cytokines [35]. There is also the potential for mixed dimer formation, or hybridization, between the synthetic TCR and the endogenous TCR, which can lead to self-reactive or non-functional TCR hybrids [36]. To avoid false positives and to prevent the chance that the endogenous TCRs would bar functional antigen-specific TCR formation at the membrane, the genes encoding the heterodimer protein would need to be knocked out. Prior studies have knocked out this gene or prevented expression through other methodologies. In one study, the constant domains of the α and β chain of the

therapeutic TCRs were swapped to prevent mispairing [37]. Another study utilized $\gamma\delta$ T cells as recipients to the therapeutic TCRs because mixed dimerization between $\alpha\beta$ TCRs and $\gamma\delta$ TCRs isn't feasible, though the *in vivo* capabilities of these cells have not yet been evaluated [37]. Other studies implemented a knockout or knockdown strategy through some form of genetic manipulation. For example, one study developed an RNAi-TCR replacement vector that silenced endogenous TCRs and expressed the therapeutic RNAi-resistant TCRs [38]. Other knockout strategies employed CRISPR-mediated gene knockouts, particularly targeting the constant regions of the α and β chains [39]. Without these proteins, there is no component to anchor the receptor to the membrane, and because the sequence is conserved amongst various antigen-specific receptors, that target is widely applicable. However, just knocking out the receptor is not enough to induce the TCR's cell killing capabilities – the CD8 coreceptor must be knocked in [40]. Whether the CD4 coreceptor interferes with TCR assemblage is unknown, but it could be similarly knocked out utilizing the aforementioned strategies.

It is important to recognize that there are two levels of TCR implementation: structural and functional. Functionality can only be achieved within a T cell line, whereas, the structural integrity of the TCR alone can be confirmed via other cell lines like HEK293. Because there is no immortalized CD8⁺ T cell line readily available on the market, the only CTLs that can be procured for research are engineered CD4⁺ T cells. These can be modified to be phenotypically similar to CD8⁺ cells. CD4⁺ helper T cells have different functions and thus different signaling capabilities/internal machinery than CD8⁺ killer T cells [41]. If one were to express a functional antigen-specific TCR along with the CD8 coreceptor, there is the chance that cytotoxic particles perforin, granzyme

B, and the cytokines stimulated from CD8+ T cell activation will not be expressible in the engineered cell line. Therefore, classic cytotoxic assays will not suffice to evaluate reactivity or functionality. Jurkat cells do secrete IL-2 upon activation, so measuring its release via ELISA assays would evaluate the functionality of the T cell receptor [42].

Gene Editing Technology

Gene editing has come a long way since its inception. Amongst the various gene editing protocols in the works, there are three that are more widely used. Programmable nucleases, namely zinc-finger nucleases, are made up of a DNA-binding domain, with two finger-like molecules designed to identify unique DNA hexamers, and a DNA cleaving domain [43]. When fused together, these essentially serve as molecular scissors, inducing double-stranded breaks at the targeted site in DNA, which are repaired via error-prone NHEJ [43]. In the absence of a repair template, this can create a non-missense or a premature stop codon, rendering the gene knocked out [44]. With a repair template, a DNA sequence can be inserted at the site of the DSBs [45]. Transcription activator-like effector nucleases (TALENs) function under the same principles. TALENs are restriction enzymes with a DNA-binding domain and a DNA-cleavage domain [46]. Much like the zinc finger nucleases, TALENs induce a double stranded break that is repaired via NHEJ or via a template containing exogenous DNA [46]. The CRISPR-Cas9 system is predominantly the same, composed of a Cas endonuclease and guide RNAs as part of the DNA-binding domain [47]. Though similar in theory, the practicality and adaptability of CRISPR-Cas9 tech make it the optimal candidate for gene knockouts – TALENs and zinc-finger nucleases require both unique nuclease selection and DNA-binding domain

designs; whereas, CRISPR-Cas9 requires only a new gRNA design for each target [48]. Additionally, CRISPR-Cas9 has been widely used to knock out endogenous TCRs in the past, meaning there are resources to draw from in repeating similar experiments [39].

How CRISPR Came About

First defined in 1987 by Yoshizumi Ishino at Osaka University, CRISPR represents a set of repetitive DNA fragments found in various bacteria species [49]. These fragments function to protect bacteria from invasive nucleic acids, storing short fragments of foreign phages previously encountered for future exposure, constituting an acquired form of adaptive immunity [50]. The short, repetitive fragments guide the Cas endonucleases (as part of the CRISPR complex) to their complementary sequences when re-exposed to induce double-stranded breaks and prevent their deleterious expression [51]. Researchers eventually discovered ways to harvest this complex to edit the human genome. In 2012, researchers observed that CRISPR could be adapted to perform DNA cleavage with the Cas9 nuclease *in vitro*, and in 2013, researchers performed genome editing using CRISPR in a mammalian cell line [47]. Now, CRISPR-mediated gene editing is considered mainstream, with over 7000 publications citing its use. With prominent ethical implications and serving as the most advanced form of genome editing, the first-ever CRISPR babies were brought to term in 2018 [52]. Through CRISPR-mediated germline editing, He Jiankui knocked out the CCR5 gene to prevent susceptibility to smallpox, cholera, and HIV [53]. This brought to light some of the potential misuses of gene editing while also serving as a testament to how advanced CRISPR technology has become [54].

There are two modes of CRISPR gene editing: non-homologous end joining (NHEJ) and homology directed repair (HDR) [55]. For the former, a double-stranded break is induced and is repaired via the error-prone NHEJ, where an insertion or deletion can disrupt the expression of a target gene [56]. With HDR, a repair template is utilized to add a given insert to the site of the break [55]. The template is composed of the insert sequence flanked by regions homologous each side of the break [57]. Because the DNA binding domain doesn't need to be bound to distinct cleaving nucleases, a testament to its adaptability, and because the cost is significantly lower, CRISPR has found itself at the forefront of gene editing.

How CRISPR Works

A CRISPR complex is made up of a guide RNA (gRNA) and an endonuclease like Cas9 [58]. gRNAs are customizable, with a pre-designed scaffold sequence and a unique spacer sequence (falling at about 20 nucleotides in length) complementary to the gene to be knocked out [58]. When the gRNA and endonuclease are joined, a conformational change takes place, allowing the newly formed ribonucleoprotein complex to bind to the target sequence [59]. Protospacer adjacent motifs (PAMs), 2-6 bp long sequences specific to the endonuclease in the complex, are what guide the ribonucleoprotein complex to the target site, serving as the signal sequence needed for the complex to bind and induce the DSB [60]. As the complex comes into contact with the target sequence and the PAM sequence that follows, the seed sequence (at the 3' end of the spacer) begins to anneal to the target – if enough homology is present, the rest of the spacer will bind the target sequence, and Cas9 will induce a double-stranded break 3-4

nucleotides upstream of the PAM [60]. This DSB will be repaired in one of the aforementioned manners, resulting in an insertion, deletion, or frameshift mutation [55].

This complex can be formed and delivered in a variety of ways. One common method of accomplishing this involves inserting the custom gRNA into a CRISPR-compatible vector containing the scaffold and Cas9 nuclease to be transfected or transduced [61]. An alternative approach to this is to deliver the RNP directly into the cell [61]. First, the RNP is formed by incubating the nuclease and gRNA together, and then the RNP is delivered directly via electroporation, via a receptor ligand that triggers endocytosis once bound to its complementary receptor, or through cationic lipid vesicles that passively cross the membrane into the cell *in vivo* [48,62,63]. Though these RNP delivery methods entail fewer steps, they are early in development.

Downsides of CRISPR

CRISPR holds great promise for gene editing, but the efficacy is clouded by its off-target effects. When the seed sequence binds to the target sequence, it recognizes enough homology for the rest of the spacer to bind and induce a DSB [60]. However, if there is enough homology with other sequences upstream of a PAM sequence in a given genome, then unintended mutations can take place [64]. This means that in addition to inducing mutations at the target sequence, a multitude of other sequences could be mutated, preventing or enabling proteins to be expressed when they shouldn't [65]. Not only could this prevent the achieved outcome, but it could also spell danger for ACT therapies, where cells with unknown mutations are being infused into human patients, or for germline gene editing, where the off-target effects could result in unintended

phenotypic consequences. Studies have observed CRISPR RNA-guided endonucleases' off-target activity in human cells conferred off-target alterations in the genome [64,65].

Experimental Design

For the purposes of this experiment, a CRISPR-Cas9 system was utilized to eliminate endogenous TCRs for downstream use in cloning antigen-specific CD8⁺ TCRs. The knockout was accomplished by designing gRNAs to target the α and β constant regions of the Jurkat TCR heterodimer, rendering the receptors unable to be expressed. These gRNAs were separately cloned into mammalian expression vectors with the pre-existing Cas9 endonuclease and scaffold sequence. Upon confirming the gRNAs were successfully cloned into the vector via Sanger sequencing, the vectors were to be transfected via electroporation and validated via antibody staining and subsequent flow cytometry analysis. Because the Jurkat cell line is CD4-positive, gRNAs were similarly designed to knock out the coreceptor, which could interfere with the cytotoxic capabilities of a synthetic CD8⁺ TCR. To confer a cytotoxic response, the CD8 coreceptor would similarly be transfected into the cell line in a mammalian expression vector. Engineering a CD4⁺ human T cell line to be CD8-positive and free of endogenous TCRs could have broad applications for ACT therapy.

METHODS – CLONING FUNCTIONAL ANTIGEN-SPECIFIC TCRS:

Antigen-Specific T Cell Expansion

Primary peripheral blood mononuclear cell (PBMC) lines were obtained from healthy donors at Baylor College of Medicine. BCP cell lines were cultured in B cell media (R&D Systems) under standard conditions and passaged prior to confluence. To promote expansion of desired antigen-specific T cell populations, APC's were pulsed with 10 μ g FluM1 peptide⁵⁸⁻⁶⁶ (GILGFVFTL, ProImmune) overnight with IL-4 (R&D Systems). The following day, IL-4 medium was removed and PBMCs were co-cultured with FluM1 peptide pulsed APCs, IL-2 (R&D Systems), and IL-7 (R&D Systems) for 12 consecutive days. 50% of media was replaced on days 5 and 10. *Created in collaboration with Nolan Vale.*

Sequencing FluM1-Specific T Cell Receptors from BCP5 Donor Cells

10*10⁶ stimulated BCP PBMCs were lysed and RNA was isolated using RNAqueous Phenol-Free RNA Isolation Kit (Invitrogen). Purified transcripts were reverse transcribed with Oligo (dT)₁₈ primers (IDT) using Superscript III Reverse Transcriptase (Invitrogen). Resultant cDNA was amplified with DreamTaq Hot Start Polymerase (Thermo Fisher) using gene-specific primers (IDT) located in variable and constant regions of $\alpha\beta$ transcripts of interest, determined by VDJdb, an online TCR chain database. Amplifications were verified via gel electrophoresis and Sanger sequencing. *Created in collaboration with Nolan Vale.*

Designing Primers with Site-Specific Attachment Sites

Primers were designed to add attB1 and attB2 site overhangs to the α and β FluM1-specific TCR sequences (Invitrogen). Using DreamTaq polymerase (and its corresponding 1-step PCR protocol), a PCR was conducted to add the attB sites (TRAV17, TRAC, TRBV19, TRBC) and amplify the sequence. The resulting lengths of the PCR product were confirmed on a 1% agarose gel and purified (SV Wizard Gel/PCR Clean-Up Kit) to be verified via Sanger sequencing. *Created in collaboration with Nolan Vale.*

Gateway Reaction

To create the pENTR vector, 150 ng of pDONR221 (Invitrogen) (100 ng/microliter) was added to 50 fmol of the purified PCR products, 6 ul of NF water, and two ul of BP Clonase II (Invitrogen). These solutions were incubated for one hour at 25 degrees Celsius, before the reaction was terminated with 1 microliter of Proteinase K (Invitrogen). Following termination, the solutions were incubated for 10 minutes at 37 degrees Celsius. To perform a colony screen, the entry vector clones were transformed into 40 ul of chemically competent DH5 α *E. coli*. Upon completion, 150 ul of the transformed cells were plated on LB agar with Kanamycin selection (50 mg/ml) and incubated at 37 degrees Celsius for 16 hours. Three colonies were taken from each plate and miniprepmed via the Plasmid Miniprep Kit (Qiagen) before being verified with Sanger sequencing. The miniprepmed product (pENTR) was diluted to 150 ng/microliter before being added 150 ng of destination vector pcDNA3.2 (Invitrogen), 6 ul of water, and 2 ul of LR Clonase II (Invitrogen). These solutions were incubated for one hour at 25

degrees Celsius, and the reaction was again terminated with 1 microliter of Proteinase K (Invitrogen). To perform the second colony screen, the destination vector clones (pDEST) were transformed into 40 ul of chemically competent DH5 α *E. coli*. 150 ul of these transformed cells were plated on LB agar with Ampicillin selection (50 mg/ml) and incubated at 37 degrees Celsius for 16 hours. Three colonies were taken from each plate and purified via the Plasmid Maxiprep Kit (Qiagen) and verified via Sanger sequencing. *Created in collaboration with Nolan Vale.*

Transfection of Mammalian Expression Vector:

The purified mammalian expression vector (pcDNA3.2) construct was diluted in a transfection buffer (RPMI) to bring the concentration of the construct to roughly 1.2 micrograms in 20 ul. Similarly, 10^7 Jurkat cells were resuspended in RPMI and harvested for each transfection sample. After placing on ice, these Jurkat cell samples were transferred to electroporation cuvettes. The constructs were added to the cell solutions and mixed. The Neon® Transfection System was used to electroporate the cells at 2150V, 20ms, 1 pulse. *Created in collaboration with Nolan Vale and Peaches Ulrich.*

Tetramer Staining and Flow Cytometry Analysis

In preparation for tetramer staining, 5 ml of H.Serum was added to 45 ml FACs buffer. To create the dasatinib mixture, 2 ul of dasatinib was added to 10 ml of the H.Serum/FACs buffer solution. The FluM1 tetramers were spun down in the cold room at 14,000g for 5 minutes. Meanwhile, the transfected cell samples were transferred from their respective wells to labeled Eppendorf tubes and centrifuged at 500 g for 6 min. 1 ml

of buffer (H.Serum/FACs) was added to each of the wells the cell samples were pulled from. After centrifugation was complete, the media was aspirated. Then, the 1ml of the H.Serum/FACs buffer that was placed in the wells was extracted, added to each centrifuged sample, mixed, and centrifuged at 500 g for 5 min. The supernatant was again aspirated, and 200 ul of dasatinib mix was added to each before incubating for 30 min at room temperature. The samples were flicked every 10-15 minutes during this period to ensure sufficient mixing. Following the incubation period, 1 ml of dasatinib mix was added to the cell samples, which were centrifuged at 500 g for 5 min. The supernatant was aspirated from these samples to leave only 100 ul of solution in each. 10 ul of the FluM1 tetramer (ProImmune) was added to each sample and mixed thoroughly. This mix was allowed to incubate for 30 minutes at room temperature in the dark (covered in foil), where they were flicked every 10-15 minutes. The resulting samples were brought up in 1 mL of FACs buffer and centrifuged at 500 g for 5 min. The supernatant was aspirated, leaving the pellet intact, and 1 ml of PBS was added. The solution was mixed and centrifuged at 500 g for 5 minutes. The supernatant was again aspirated, and the pellet was resuspended in 1 ml of PBS. Flow cytometry analysis was conducted with the tetramer-stained samples. *Created in collaboration with Peaches Ulrich.*

METHODS – CRISPR TCR KNOCKOUT:

Guide RNA Design

The CD4⁺ Jurkat T cell line was gifted from ATCC. The cells were lysed and RNA was isolated using RNAqueous Phenol-Free RNA Isolation Kit (Invitrogen). Purified transcripts were reverse transcribed with Oligo (dT)₁₈ primers (IDT) using Superscript III Reverse Transcriptase (Invitrogen). The resulting cDNA was amplified with DreamTaq Hot Start Polymerase (Thermo Fisher) using gene-specific primers (IDT) located in variable and constant regions of $\alpha\beta$ transcripts of interest. The PCR products were purified (SV Wizard Gel/PCR Clean-Up Kit) and verified via Sanger sequencing. Utilizing prior literature, the variable, joining, and constant region of the Jurkat TCR sequence were annotated. gRNAs were designed to target the constant regions of the α and β chain utilizing the IDT Custom Alt-R CRISPR-Cas9 guide RNA design tool. Based on the off-target and on-target analysis provided, two gRNA designs were chosen for both the α and β chains. These gRNA designs were used to create complementary oligos with the necessary typeIIIs restriction sites for double-stranded synthesis in the Golden Gate-compatible PX458 vector.

Phosphorylation of Oligos

Before annealing the oligos, 1 ul of the sense and antisense strands were added to an Eppendorf tube, followed by 1 ul of 10x ligation buffer, 0.5 ul of PNK (10/microliter) (New England BioLabs), and 6.5 ul of NF water. The phosphorylated strands were stored at -20 degrees Celsius.

Annealing Oligos

The thawed phosphorylated strands were placed in a hot water bath at 95 degrees Celsius for 5 minutes. The samples were allowed to cool to room temperature before being stored at -20 Celsius. To confirm that the oligos were effectively annealed, 1 ul of ethidium bromide was mixed with 4 ul of the annealed oligo sample and run on a 3% agarose gel.

Cultivating Mammalian Expression Vector PX458

The agar stab of the pSpCas9(BB)-2A-GFP (PX458) vector gifted by the Feng Zhang lab was used to streak three ampicillin agar plates (50 mg/ml). They were incubated at 37 degrees Celsius for 16 hours, and two colonies were chosen from each to inoculate overnight cultures. To prepare the overnight cultures, a pipette tip with the chosen colonies were added to 7 ml of LB broth and 7 ul of ampicillin antibiotic. The following samples were shaken for 17 hours, before a miniprep was performed with the Plasmid Miniprep Kit (Qiagen). The miniprepped products were confirmed via Sanger sequencing utilizing the U6 promoter universal primer (LKO.1 5') (IDT). The overnight cultures were also used to make glycerol stocks, where 500 ul of culture was added to 500 ul of 80% glycerol solution and stored at -80 degrees Celsius.

Golden Gate Reaction

To integrate the gRNAs into the PX458 vector, 25 nanograms of the purified vector was added to 1 ul of the annealed oligos (10 micromolar), followed by 1 ul of 10x T4 ligation buffer, 0.5 ul of BbsI restriction enzyme, 0.5 ul of T4 DNA ligase (400 U/microliter), and 7 ul NF water (New England BioLabs). The resulting samples were incubated in a

thermocycler, alternating between 37 degrees Celsius for 5 minutes and 23 degrees Celsius for 5 minutes for 25 cycles. These products were transformed into 50 ul of chemically competent DH5 α *E. coli*, plated on ampicillin agar plates (50 mg/ml), and incubated at 37 degrees Celsius for 17 hours. A colony PCR using the DreamTaq HS enzyme was performed with universal U6 promoter primer (LKO.1 5') and reverse primers (CS1, CS2) customized to PX458 vector's BbSI restriction sites (IDT) (Supp. Table 3, 4). Meanwhile, 2 colonies were chosen from each plate to inoculate overnight cultures. The cultures, after being incubated and shaken for 17 hours, were utilized to make glycerol stocks (to be stored at -80 degrees Celsius) and to purify the vector via the Plasmid Miniprep Kit (Qiagen). The resulting product was sent for Sanger sequencing.

Transfection of PX458 Vector

The purified PX458-gRNA construct was diluted in a transfection buffer (RPMI) to bring the concentration to roughly 1.2 micrograms in 20 ul of NF water. Similarly, 10^7 Jurkat cells were resuspended in RPMI and harvested for each transfection sample. After placing on ice, these Jurkat cell samples were transferred to electroporation cuvettes. The constructs were added to the cell solutions and mixed. The Neon® Transfection System was used to electroporate the cells at 2150V, 20ms, 1 pulse.

Antibody Staining and Flow Cytometry Analysis

In preparation for flow cytometry analysis, the Jurkat antibodies were vortexed and spun down. The transfected cell samples were transferred from the wells to labeled Eppendorf tubes and centrifuged at 500 g for 5 min. In the meantime, 1 ml of buffer (FACs/MACs)

was added to each well the sample was pulled from. After centrifugation was complete, the supernatant was aspirated, and the 1ml of buffer that was added to each well was extracted and added to the cell samples. The samples with the newly-added buffer were mixed and centrifuged at 500 g for 5 min. While the samples were centrifuging, the antibody master mix was prepared (1ul CD8PC5/per sample, 1ul CD14-FiTC/per sample, 1ul CD19-FiTC/per sample) (ProImmune). After centrifugation, the supernatant was aspirated, leaving the pellet undisturbed. Then, the antibody mixture was vortexed, and 100 ul were transferred to each sample. Upon thorough mixing, the samples were allowed to stain for 30 minutes on ice in the dark (covered in foil), where the samples were flicked every 10-15 minutes to increase staining efficiency. After the incubation period, the stained samples were brought up in 1 ml of PBS and centrifuged. After the final centrifugation was performed, the pellet was resuspended in 600 ul of PBS, and the samples were placed on ice in the dark until flow cytometry analysis. Finally, flow cytometry analysis was performed.

MGH CRISPR Sequencing

To prepare samples to be sent to the MGH CRISPR Sequencing core, a number of steps needed to be completed. Primers were designed to encompass an amplicon within the Jurkat genome. This amplicon, which needs to fall between 200 and 600 bp long, includes the CRISPR cut site in the first 100 base pairs along with the target site. To gain this PCR product post-transfection, RNA was first isolated using a RNAqueous Phenol-Free RNA Isolation Kit (Invitrogen). The purified transcripts were reverse transcribed with Oligo (dT)₁₈ primers (IDT) using Superscript III Reverse Transcriptase (Invitrogen),

and the resulting cDNA was amplified with DreamTaq Hot Start Polymerase (Thermo Fisher) in a PCR reaction using primers designed to amplify and isolate the desired amplicon (IDT). To characterize the PCR product, a 1% agarose gel was performed. To remove any contaminants from the product, the PCR products were purified with the SV Wizard Gel/PCR Clean-Up Kit. Upon confirming the lengths, the samples were nanodropped to ensure the concentration fell between 10 and 40 ng/microliter. Finally, 35 ul of each sample were aliquoted to be sent to the MGH CRISPR Sequencing Core, along with a visualization of the gel and the corresponding concentration values.

RESULTS:

Cloning FluM1-Specific T Cell Receptors

Via Sanger sequencing technology, the homology between the Gateway cloning intermediates was evaluated for FluM1-specific α and β TCR sequences extracted from donor PBMCs. Derived from literature and seen in high frequency in TCR database VDJdb, the chosen TCR α sequence contained variable region 17-01 (TRAV17*01), joining region 43-01 (TRAJ43*01), and the α chain constant region (TRAC) (Fig. 1). The TCR β sequence contained TCR β variable region 19-01 (TRBV19-01), domain region 2-02 (TRBD2*02), joining region 2-1-01 (TRBJ2-1*01), and the beta chain constant region (TRBC) (Fig. 2). Homology between the TCR sequence in pDONR221, pcDNA3.2, the maxiprepped destination vector was evaluated to be >90% (Fig. 1, 2).



Figure 1: Annotated Sanger sequencing results for the TCR α sequence in A) pDONR221 B) pcDNA3.2 and C) the maxiprepped expression vector. The variable region (TRAV17-01), joining region (TRAJ43-01), and constant region (TRAC) were used to evaluate homology throughout the cloning process. *Developed in collaboration with Nolan Vale*



Figure 2: Annotated Sanger sequencing results for the TCRβ sequence in A) pDONR221 B) pcDNA3.2 and C) the maxiprepped expression vector. The variable region (TRBV19-01), domain region (TRBD2-02), joining region (TRBJ21-01), and constant region (TRBC) were used to evaluate conservation of sequence. *Developed in collaboration with Nolan Vale.*

Flow Cytometry Analysis of KSA FluM1 Clone in NonA2 Donor PBMCs

As part of a separate venture, the KSA FluM1-specific TCR was cloned, transfected into NonA2 PBMCs, and stained with FluM1 tetramers. To determine proper assembly at the membrane and a degree of functionality measured by binding affinity, flow cytometry analysis was performed. In an A2 donor that is likely Flu-positive, there would be no way to confirm the binding affinity exists between the tetramer and the synthetic construct. Utilizing a non-A2 donor, the FluM1 tetramer's only opportunity to bind would be to the FluM1-specific TCR. It was observed that there was

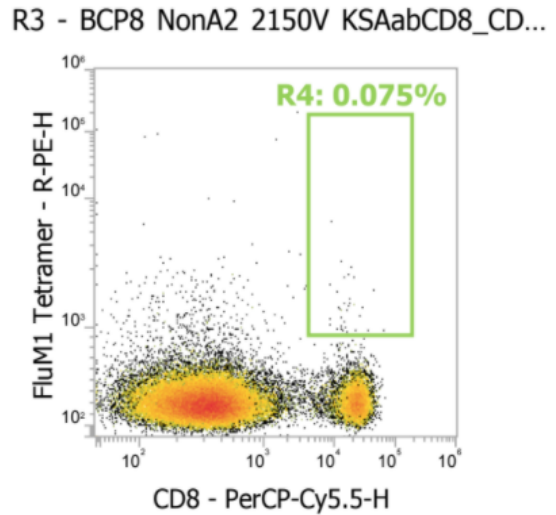


Figure 3: Flow cytometry analysis of FluM1 tetramer binding affinity to the FluM1-specific TCR construct in nonA2 PBMCs. Constructs containing the FluM1-specific TCRs were transfected into NonA2 PBMC donors and stained for flow cytometry analysis.

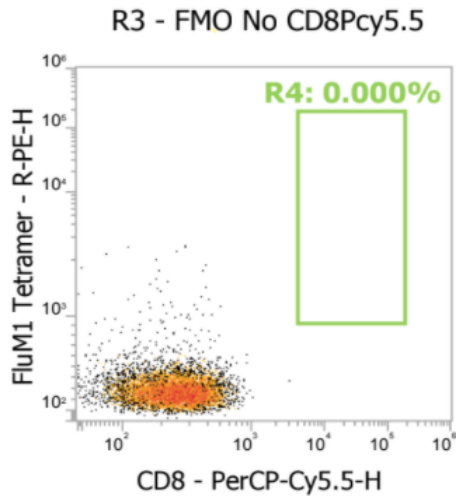


Figure 4: Flow cytometry analysis of FluM1 tetramer affinity to the FluM1-specific TCR construct (negative control). Constructs containing the FluM1-specific TCRs were transfected into PBMC donors and stained for flow cytometry analysis.

binding between the tetramer and the construct (Fig. 3). Serving as a negative control, the same was accomplished but in cells without the coreceptor CD8. There was no binding affinity in the absence of CD8 observed in flow cytometry analysis (Fig. 4).

Annotated Jurkat TCR Sequences:

Using prior studies that characterized and paired high frequency FluM1-specific TCR α and β chains, primers were designed to amplify these regions from the cDNA samples in the immortalized CD4+ Jurkat cell line. The variable (TRAV), joining (TRAJ), and constant (TRAC) sequence were consistent with the length and nucleotide content found in past studies (Fig. 5).

Validated Jurkat TCR Sequence – Alpha Chain

GCCAGTCGGTGACCCAGCTTGGCAGCCAGTCTCTGTCTCTGAAGGAGCCCTGGTTCTGCTGAGGTGCAACTACTCATCGTCTGTTCCACCATATC
 TCTTCTGGTATGTGCAATACCCCAACCAAGGACTCCAGCTTCTCCTGAAGTACACATCAGCGGCCACCCTGGTTAAAGGCATCAACGGTTTTGAGGC
 TGAATTTAAGAAGAGTGAAACCTCCTTCCACCTGACGAAACCCCTCAGCCCATATGAGCGACGCGGCTGAGTACTTCTGTGCTGTGAGTGAAGGGTA
 CAGCAGTGCTCCAAGATAATCTTTGGATCAGGGACCAGACTCAGCATCCGGCCA Aatatacagaacctgacctgacctgtaccagctgagagacttaaatccagtg
 caagtctgtcctattcacgatttgatttcaaacaaatgttcacaaagtaaggattctgatgtatatacagacaaaactgtctagacatgaggtctatggactcaagagcaacagctgtggtc
 ctggagcaacaatctgacttgcagtgcaaacgcttcaacaacagcattattccagaagacaccttctcccagcccagaagtctctgtgatgcaagctggcagagaaagcttgaacagatac
 gaacataaacttcaaacctgtcagtgattgggtccgaatcctcctgaaagtggcgggttaactctgctatgacgctgctggctgtgtccagctgagactctcaagattgaagacagctgtgctc
 cctcctcctcctctgcatggcctctctcctcctcaaacagaggaactcctccaccccaaggaggtaagctgtaccacctgtgccccccgcaatgccaccaactggatggatcctacc
 cgaatttatgattaagctgctgaagagctccaacaactgtgccccctctgttccctattgctgtctgactgacctgacatcacggcagagcaaggctgtgagcctccctgtgctgacat
 tccctcctgctcccagagactcctccgcatcccacagatgatgatcctcagtggttctctggctctagctctgagaaatgttgagggttatttttttaagtggtcataaagaaatacatagtat
 tcttcttcaagacgtgggggaataatctcattatcgaggcctgtatgtgtgtctgtggcgtgtgtatgtctctgctgcccgatgcctc

Key:
 TRAV
 TRAJ
 TRAC

Validated Jurkat TCR Sequence – Beta Chain

GATGCTGGAGTTATCCAGTCACCCCGCCATGAGGTGACAGAGATGGACAAGAAGTGACTCTGAGATGTAAACCAATTCAGGCCACAACCTCCC
 TTTTCTGGTACAGACAGACCATGATGCGGGGACTGGAGTTGCTCATTACTTTAAACAACAACGTTCCGATAGATGATTCAGGGATGCCCGAGGAT
 CGATTCTCAGCTAAGATGCCTAATGCATCTTCCACTCTGAAGATCCAGCCCTCAGAACCAGGGACTCAGCTGTGACTTCTGTGCCAGCAG
 TTTAGCCTAACTATGGCTACACCTCGGTTCCGGGGACCAGGTTAACCGTTGTAGgaggacctgaaaaactgttcccaccgaggtcgtgtgttgagccatcagaag
 cagagatctcccacacccaaaggccacactggatgctggccacaggtcttaccaccgaccagtgagctgagctgtgtgggtgaatgggaagggtgcacagtggggtcagcacagacc
 cgcagcccccaaggagcagcccgcctcaatgactccagatactgctgagcagccgctgagggctcggccacctctggcagaacccccgaaccacttccgctgcaagtcagttctacg
 ggtcctcggagaatgacgagtgaccagatagggccaaacccgtcaccagatgctcagcgcgagggcctggggtagagcagactgtggcttaccctcagatctaccagcaagggtcct
 gctgcccacatcctctatgagactctgtaggggaaggccactgtatgctgtgtgtcagtgccctgctgtatggcctatggtcaagagaaggattccagaggc

Key:
 TRAV
 TRAJ
 TRAC

Figure 5: Validated Jurkat TCR sequence for α and β chains. The sequences, derived from prior literature, were annotated to include the variable region (TRAV), joining region (TRAJ), and the constant region (TRAC), consistent with prior findings.

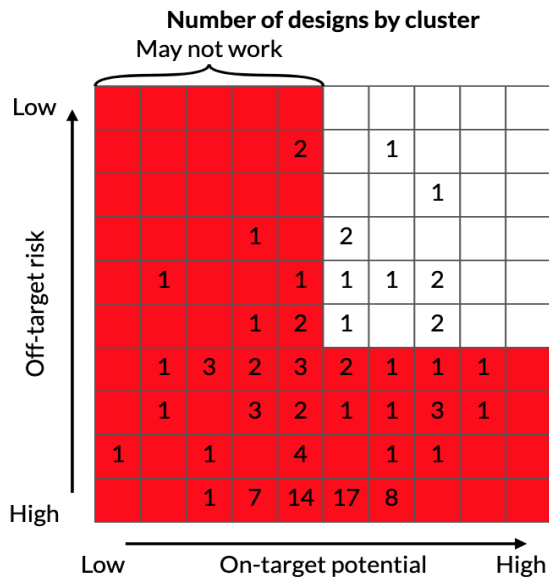
Guide RNA Design for α Chain

Utilizing designs generated from the IDT Custom Alt-R CRISPR-Cas9 guide RNA design tool, four gRNAs compatible with the constant region of the α chain were chosen for further analysis. Two were selected for their high on-target/off-target score to be utilized for CRISPR-Cas9 knockout system (Fig. 6). TypeIIIs restriction sites complimentary to the PX458 vector were added to the gRNA designs for Golden Gate cloning (Supp. Table 1).

No.	gRNA Sequences (Alpha)	PAM Sequence	On-Target Score	Off-Target Score
1	(G)AAGTTCCTGTGATGTCAAGC	TGG	78	60
2	(G)TTCGGAACCCAATCACTGAC	AGG	80	77
3	(G)CTCGACCAGCTTGACATCAC	AGG	63	81
4	(G)TCTTCTTCTCAAGACGTGGG	TGG	63	59

Figure 6: gRNA designs curated from the IDT Custom Alt-R CRISPR-Cas9 guide RNA design tool for the constant region of the α chain of the endogenous Jurkat TCR, the associated PAM signal sequence, and off-target/on-target score. Bolded sequences were ordered for experimental purposes [104].

There were 100 gRNAs curated by the IDT Custom Alt-R CRISPR-Cas9 guide RNA design tool for targeting the constant region of the α chain. High off-target risk or low binding potential classified 89 gRNAs as unlikely to work effectively as part of the CRISPR-Cas9 system (Fig. 7). Of the 11 that were classified as effective, only four were



chosen due to their placement in the clustered matrix (Fig. 6). The gRNAs selected were designed to target the region 300-400 bp downstream of the TCR joining region (TRAJ) (Fig. 8).

Figure 7: Designs curated by IDT Custom Alt-R CRISPR-Cas9 guide RNA design tool (for the α constant region and their relative on-target potential and off-target risk. The red zones indicate gRNA designs that have a higher chance of not working effectively as part of the CRISP-Cas9 complex [104].

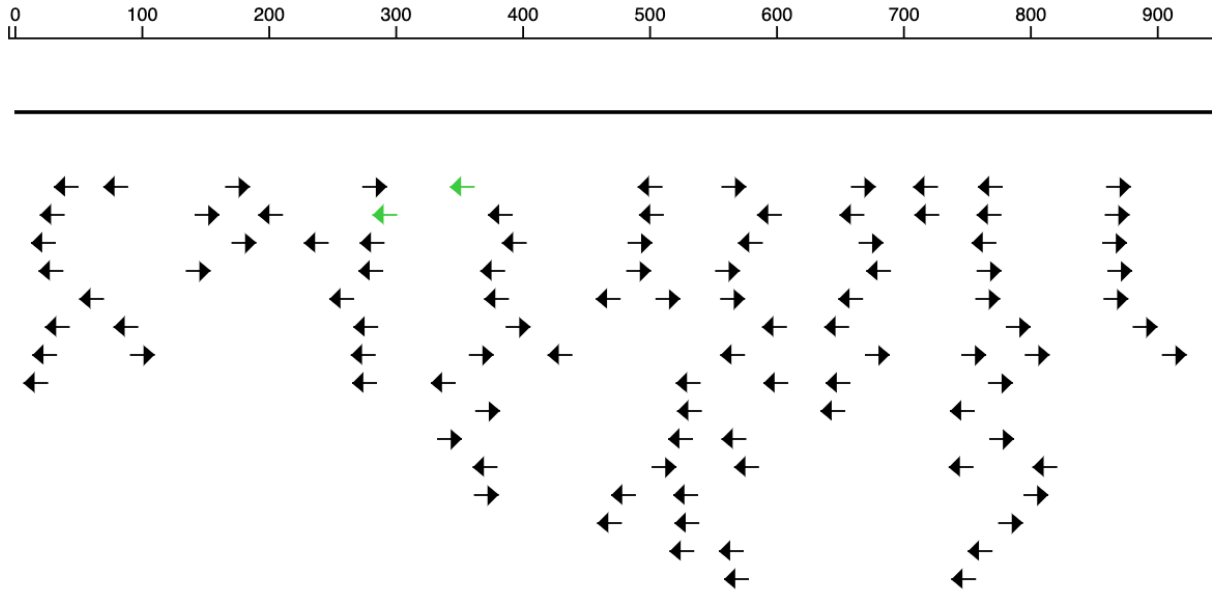


Figure 8: The location and orientation of the customized Jurkat TCR α chain gRNAs curated from the IDT Custom Alt-R CRISPR-Cas9 guide RNA design tool. 100 gRNAs were designed from the provided constant region. There appeared to be no correlation between orientation or generalized location and high off-target/on-target score [104].

Guide RNA design for β Chain

Utilizing designs generated from the IDT Custom Alt-R CRISPR-Cas9 guide RNA

design tool, four gRNAs compatible with the constant region of the β chain were chosen

for further analysis. Two were selected for their high on-target/off-target score to be

utilized for the CRISPR-Cas9 knockout system (Fig. 9). TypeIIIs restriction sites

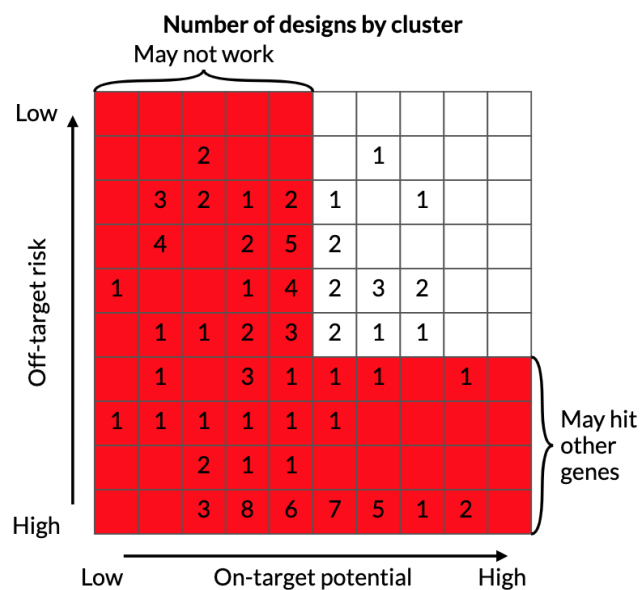
complimentary to the PX458 vector were added to the gRNA designs for Golden Gate

cloning (Supp. Table 2).

No.	gRNA Sequences (Beta)	PAM Sequence	On-Target Score	Off-Target Score
1	(G)AGGCTTCTACCCCGACCACG	TGG	63	83
2	(G)GACCAGCACGGCATAACAAGG	TGG	73	74
3	(G)CCGACCACGTGGAGCTGAGC	TGG	73	58
4	(G)TCAAACACAGCGACCTCGGG	TGG	57	80

Figure 9: gRNA designs curated from the IDT Custom Alt-R CRISPR-Cas9 guide RNA design tool for the constant region of the β chain of the endogenous Jurkat TCR, the associated PAM signal sequence, and off-target/on-target score. Bolded sequences were ordered for experimental purposes [104].

There were 100 gRNAs curated by the IDT Custom Alt-R CRISPR-Cas9 guide RNA design tool for targeting the constant region of the β chain. High off-target risk or low binding potential classified 84 gRNAs as unlikely to work effectively as part of the CRISPR-Cas9 system (Fig. 10). Of the 16 that were classified as effective, only four



were chosen due to their placement in the clustered matrix (Fig. 9). The gRNAs selected were designed to target the region about 100 bp and 450 bp downstream of the TCR joining region (TRAJ) (Fig. 8).

Figure 11: Designs curated by IDT Custom Alt-R CRISPR-Cas9 guide RNA design tool for the β constant region and their relative on-target potential and off-target risk. The red zones indicate gRNA designs that have a higher chance of not working effectively as part of the CRISPR-Cas9 complex [104].

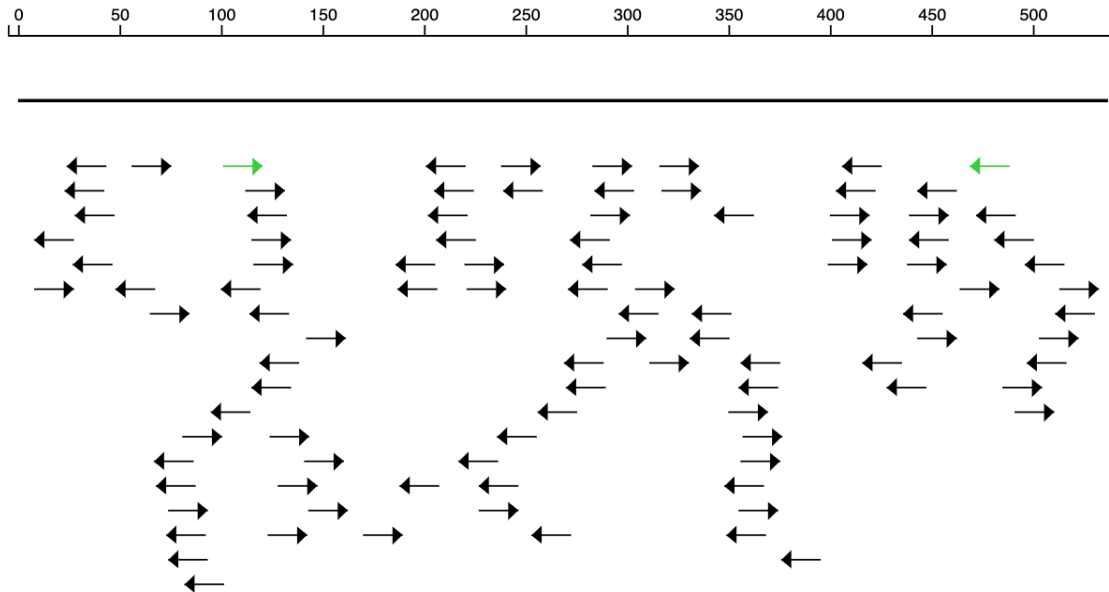


Figure 12: The location and orientation of the customized Jurkat TCR β chain gRNAs curated from the IDT Custom Alt-R CRISPR-Cas9 guide RNA design tool. 100 gRNAs were designed from the provided constant region. There appeared to be no correlation between orientation or generalized location and high off-target/on-target score [104].

Confirmation of Double-Stranded Synthesis of Guide RNAs

To evaluate whether the sense strand and antisense strand of the complimentary gRNA strands were phosphorylated and annealed effectively, the annealed strands and just the sense strand of each gRNA design were run on a 3% ethidium bromide gel. Because EtBr has a greater affinity to double-stranded DNA and because double-stranded DNA is linearized in PCR reactions, it was expected that annealed oligos would be brighter and longer (about double in length) than the sense strand.

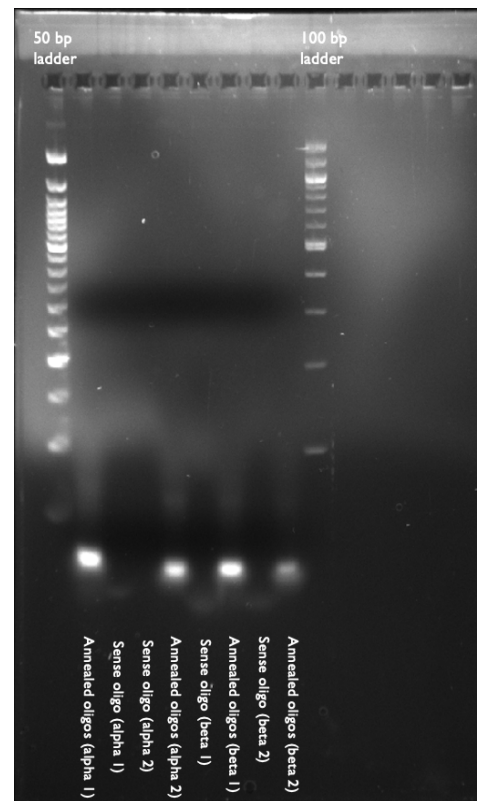


Figure 13: Annealed gRNA oligos relative to the sense strand of the double-stranded gRNAs run on a 3% ethidium bromide gel.

It was observed that the annealed oligos were about double the length of the sense strands and significantly brighter (Fig. 13).

Confirming Integration of Guide RNAs into PX458

Utilizing Golden Gate cloning, the annealed oligos were integrated into the PX458 vector. To confirm that the gRNA inserts were effectively recombined into the vector, the universal U6 promoter primer (LKO.1 5'), falling upstream of the first BbSI site, and custom reverse primers (CS1 and CS2) designed just outside the second BbSI restriction site were used in a PCR reaction to amplify the gRNA inserts (Supp. Table 3, 4). The expected lengths of the gRNA inserts were ~180 bp. The actual length of the amplified gRNA inserts for PCR reactions using the CS2 reverse primer was 180 bp, while there was no visible band for the gRNA inserts for PCR reaction using the CS1 reverse primer (Fig. 14).

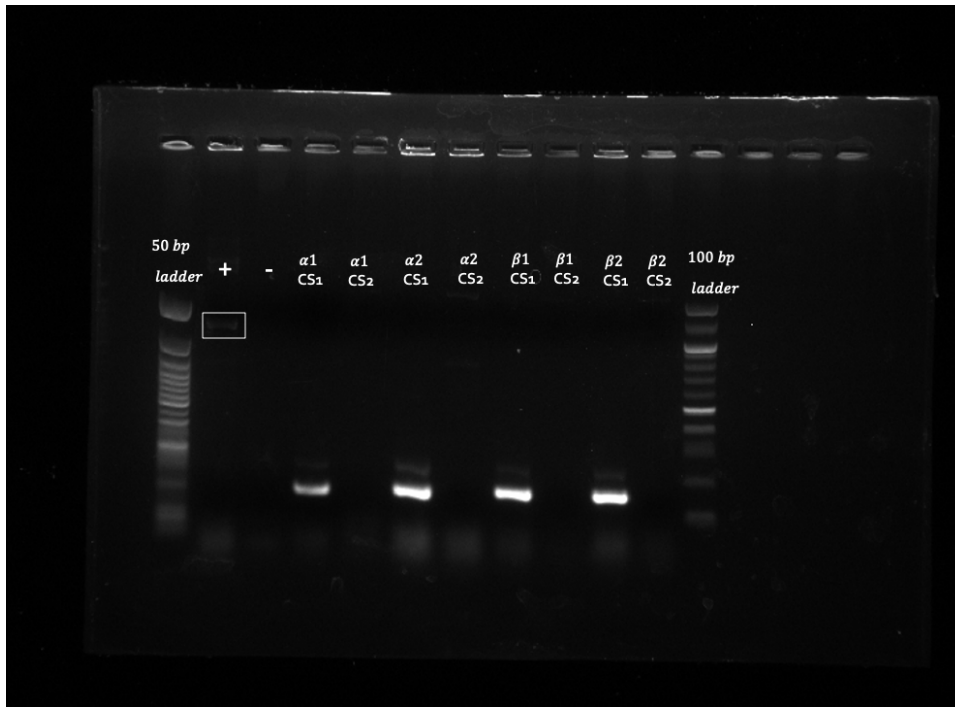


Figure 14: Amplification of α and β gRNA inserts in the PX458 vector. The constructs were isolated and amplified via customized reverse primers (CS1 and CS2) and the universal forward primer for the U6 promoter (LKO.1 5').

Validation of Guide RNAs in PX458

The PX458 constructs were sent for Sanger sequencing to confirm that the gRNA inserts were successfully integrated into the vector. In sequencing the β chain, the gRNA sequence was only retrieved from sequencing results utilizing the forward U6 promoter primer (LKO.1 5') (Fig. 15). Conversely, in sequencing the α chain, results were only retrieved from sequencing results utilizing the CS2 reverse primer (Fig. 15). There was 100% homology between the original gRNA designs and those in the construct (Fig. 15).

gRNA Alpha Chain (1)

```
CATGGTTATGTCATATACCTACTGACTCAAGCTGCAGTTGACGGATCTAGGTGAAATCCCTCTGGGATAATGCATGAGCAAAAATCCATAACCGTGAGTTTC
GGTCCCAATCGAGGCGTACAGCCCGTTAGATAAAGATCAAGATCTCTTGAGATCCCTTTTTCTGGCGGTAATCGTCTTGGCAAAAACCCCGCTAC
CAGCGGTGTTTTGTTGCCGGATCAAGAGCTAACCAACTCCTTTTTCCGAAAGTAACTGGTTTACGACGAGCGCAGATACCAAATCTGTTCTTAGTGTAGCCGTAGTTA
GGGCCACCCTTCAAGAAGCTGTAGACCAGCCGTACATACCTCGCTCGCTAATCCTGTTACAGAGTGGCTGCTGCCAGTGGCGATAAGTCTGTCTTACCGGGTTGAACT
CAAGACGATAGTTACCGGATAAGGCGACCGAGTGGGGTGAACGGGGGGTTCGTGCACACAGCCACAGTTGGAGCGAAGCACTACACCGAACTGAGATACCTACAG
GTGAGCTATGAAGAAGCCAGCGTCCCGAAGGAGAAAGGCGGACAGGTATCCGGTAAGCGCAGGGTCCGGAACAGGAGAGCGACAGGGAGCTCCAGGGGGA
AACGCTGGTATTTATAGCTGTGCGGTTTCGCCACCTCTGACTTGAGCGTCAATTTTTGTGATGCTCGTCAAGGGGGGGGAGCCTATGGAAAAACGCGACAGCC
GGCTTTTTACGGTCTCGGGCTTTGGCGCTTTTGCTACATGTGAGGGCTATTTCCCATGATCTTCATATTTGCATATACGATACAGGCTGTAGAGAGATATT
GGAATTAATTTGACTGTAACCAAGATATTAGTACAAAATACGTGACGTGAAAGTAAATTTCTGGGTAGTTTGCAGTTTAAATATGTTTTAAATGGACTATC
ATATGCTTACCGTAACTTGAAGATTTTCGATTTCTGGCTTATATATCTTGGAAAGGACGAAACACCGAAGTCTGTGATGTCAAGCGTTTAGAGCTAGAAATAGCA
AGTAATAAGCTGGCCCCGTC
```

Key:

gRNA

gRNA Alpha Chain (2)

```
GACGTTACAGACCTAGCTTAATTCGATAACTTAGATTGATTCAAACTCTTTTAGCTAACCGGAATCTACGTGGCAAGGATTCCTGTGATCTCATGGACC
AAAATCCCTTAAACGTGAGTTTCGTTCCACTGAGCGTCAAGCTCCGTAAGAAAAGGATCAAAGGATCCCTTGGATCCCTTTTTCTGGCGTAAATCTGCG
TGCTTGGCAACAAAAAAACCCCGCTACAGCGGTGGTTTTGTTGGCGGATCAAGAGCTCAACACTCTTTTTCCGAAAGGTAAGTGGCTTACGAGCAGC
GCAGATACCAAACTGCTTATAGTGTAGCCGTAGTTAGGCCACCACTTCAAGAACTCTGTAGCACCGCTACATACCTCGCTCTGTAATCTGTTACCAAGTG
GCTGCTGCCAGTGGCGATAAGTCTGTCTTACCGGGTTGGACTCAAGACGATAGTTACCGGATAAGGCGCAGCGGTGGGCTGAACGGGGGTTCTGTGCACA
CAGCCAGCTTGGAGCGAAGCAGCTACACCGAACTGAGATACCTACAGCGTGAAGTATGAGAAAGCCACGCTTCCGAAAGGAGAAAGCGGACAGGTA
TCCGGTAAGCGCAGGCTCGAAGACAGAGAGCGCAGGAGGAGCTCCAGGGGAAACCGCTGGTATTTTATAGCTGTGCGGGTTTCGCCACCTCTGACT
TGAGCTGCTGATTTTTGTGATCTGCTCAGGGGGGGGAGCCTATGGAAAAACGCGACGCAAGCGGGCTTTTTACGGTTCTTGGCTTTTGTGGCTTTTGTGCT
CACATGTGAGGGCTATTTCCCATGATTCCTCATATTTGCATATACGATACAAAGGCTGTAGAGAGATAATTGGAATTAATTTGACTGTAAACACAAAGATATTAG
TACAAAAATACGTGACGTAGAAAGTAATAATTTCTGGGTAGTTTGCAGTTTTAAATATGTTTTAAATGGACTATCATGCTTACCGTAACTTGAAGATTTTCG
ATTTCTTGGCTTATATATCTTGTGGAAAGGACGAAACACCGTTCGGAACCCAACTCACTGACGTCTAGAGCTAGAAATAGCAAGTAACTAGCCTTCCCCC
```

gRNA Beta Chain (1)

```
NNNNNNNNNNNGCTTNTATCTTGTGGAAAGGANGAAACACCGAGGCTTCTACCCGACACGNNNTTAGAGCTAGAAATAGCAAGTTAAATAAGGCTA
GTCCGTTATCAACTGAAAAAGTGGCCAGCGAGTGGTCTTTTTGTTTGTAGAGCTAGAAATAGCAAGTTAAATAAGGCTAGTCCGTTTTTAGCGGTGCCG
CAATTCTGCAGACAATGGCTTAGAGGTACCCGTTACATAACTTACGTTAAATGGCCCGCTGGCTGACCGCCCAACGACCCCGCCATTGACGCTCAATA
TTAACGCCAATAGGACTTTCCATTGACGCTAATGGTGGAGTATTACGGTAAACTGCCCCTTGGCAGTACATCAAGTGTATCATATGCCAAGTACGCCCC
CTATTGACGTCAATGACGTTAAATGGCCCGCTGGCATTGTGCCAGTACATGACCTTATGGGACTTCTCTACTTGGCAGTACATCTACGTATTAGTACGCT
ATTACCATGGTGGAGGTGAGCCCACTGCTTCACTCTCCCCTCTCCCGCCCTCCCAACCCCAATTTGTATTATTATTTTAAATATTTTGTGCGAG
CGATGGGGCGGGGGGGGGGGGGGGGGGGNNNNNNNNNNNTGNNNNNNNNNNNNNNNNNNNNNNNNNNNNNNNNNNNNNNNNNNNNNNNNNNNNNNNN
NNNNNNNNNNNNNNNNNNNNNNNNNNNNNNNNNNNNNNNNNNNNNNNNNNNNNNNNNNNNNNNNNNNNNNNNNNNNNNNNNNNNNNNNNNNNNNNN
NNNNNNNNNNNNNNNNNNNNNNNNNNNNNNNNNNNNNNNNNNNNNNNNNNNNNNNNNNNNNNNNNNNNNNNNNNNNNNNNNNNNNNNNNNNNNNNN
NNNNNNNNNNNNNNNNNNNNNNNNNNNNNNNNNNNNNNNNNNNNNNNNNNNNNNNNNNNNNNNNNNNNNNNNNNNNNNNNNNNNNNNNNNNNNNNN
```

Key:

gRNA

gRNA Beta Chain (2)

```
NNNNNNNNNNNNNGCTTNTATCTTGTGGAAAGGANGAAACACCGGACGACGCGCATAAGGNTTTTAGAGCTAGAAATAGCAAGTTAAATAAGGCT
AGTCCGTTATCAACTGAAAAAGTGGCCAGCGAGTGGTCTTTTTGTTTGTAGAGCTAGAAATAGCAAGTTAAATAAGGCTAGTCCGTTTTTAGCGGTGCCG
CAATTCTGCAGACAATGGCTTAGAGGTACCCGTTACATAACTTACGTTAAATGGCCCGCTGGCTGACCGCCCAACGACCCCGCCATTGACGCTCAATAG
TAACGCCAATAGGACTTCCATTGACGCTAATGGTGGAGTATTACGGTAAACTGCCCTTGGCAGTACATCAAGTGTATCATATGCCAAGTACGCCCCCTA
TTGACGCTCAATGACGTTAAATGGCCCGCTGGCATTGTGCCAGTACATGACCTTATGGGACTTCTCTACTTGGCAGTACATCTACGTATTAGTACGCTATTAC
CATGTTGCGAGGTGACGCCACGTTCTGCTCACTCTCCCATCTCCCGCCCTCCCAACCCCAATTTGTATTATTATTTTAAATATTTTGTGCAAGGATGG
GGGCGGGGGGGGGGGGGGGGGNNNNNNNNNNNNNNNNNNNNNNNTGNTCNCNNNNNNNGANNNNNNNNNNNNNNNNNNNNNNNNNNNNNNNNNNNN
NNNNNNNNNNNNNNNNNNNNNNNNNNNNNNNNNNNNNNNNNNNNNNNNNNNNNNNNNNNNNNNNNNNNNNNNNNNNNNNNNNNNNNNNNNNNNNNN
NNNNNNNNNNNNNNNNNNNNNNNNNNNNNNNNNNNNNNNNNNNNNNNNNNNNNNNNNNNNNNNNNNNNNNNNNNNNNNNNNNNNNNNNNNNNNNNN
NNNNNNNNNNNNNNNNNNNNNNNNNNNNNNNNNNNNNNNNNNNNNNNNNNNNNNNNNNNNNNNNNNNNNNNNNNNNNNNNNNNNNNNNNNNNNNNN
NTNNNNNNNNNNNNNNNNNNNNNNNNNNNNNNNNNNNNNNNNNNNNNNNNNNNNNNNNNNNNNNNNNNNNNNNNNNNNNNNNNNNNNNNNNNNNNN
```

Figure 15: Annotated Sanger sequencing results for the PX458 and the α and β chain gRNA inserts. The β chain sequences were retrieved using the U6 universal forward primer (LKO.1 5') while the α chain sequences were retrieved using the custom reverse CS2 primer.

DISCUSSION:

Solving Cancer Through a Modern, Alternative approach

Cancer is the source of profound biological questions, providing insight into how cells communicate and what happens when they deviate from normal, “healthy” cell standards. But cancer isn’t just a reflection of biological principles – it’s a leading cause of death across the globe [66]. Its high incidence and the difficulty in treating it makes it a prominent point of interest in research. For years, chemotherapy and radiation have been the standard-of-care treatments, but cancer requires more than one approach. As a result, researchers and clinicians are learning to see cancer through a new lens. Instead of fighting it with toxic, foreign agents that simultaneously put patients at risk of other health complications, they are devising ways to upregulate pre-existing signaling pathways or engineering cells to better combat cancer growth. Among these strategies, there is adoptive cell transfer, where immune cells are extracted and amplified or modified to exhibit more efficient cancer killing capabilities [67].

Adoptive Cell Transfer

Adoptive cell transfer is a promising avenue for cancer therapy, involving either the expansion of pre-existing antigen-specific immune cells or the engineering of immune cell lines themselves [6]. Engineering immune cells is meant to bolster a patients’ response to the cancer cell – this can be accomplished by cloning immune receptors that will recognize and induce cell killing at the tumor site. This is a lofty goal, however, as the immune system and its associated cells make up a complex network of signaling and can be highly specific to the individual [68]. To mediate this understanding,

the immune system can be split into two interdependent arms: the innate and adaptive [69]. The innate immune system accounts for any physical barriers (such as skin), defense mechanisms (such as secretions), and recognition/signaling from innate immune cells (including macrophages, monocytes, and neutrophils) [70]. These innate immune mechanisms are functionally the same among subjects, but adaptive immune responses, which are mediated by B and T cell lymphocytes, are dependent on a person's exposure and recognition of specific antigens [71]. Upon recognizing antigens presented on the cell surface, T and B cells mount an antigen-specific response to clear the body of infection while conferring long-term immunity through the proliferation of memory B and T cells [71]. Not only does a person's exposure to pathogens dictate their unique immune response, but the receptors responsible for recognizing these antigens, the MHC (or HLA molecules), are also not conserved amongst individuals, leaving some populations more susceptible to infections or autoimmune disorders than others [72]. Different individuals respond to cancer differently for these reasons, so it makes sense to customize the treatment to the nature of a given patient's immune system and cancer subtype. The programmability of adoptive cell transfer is a means to do this. The quantity and type of immune cell being administered to the patient is in the hands of the clinicians, and though this can be dangerous if performed wrong, it provides a more adaptable, specific treatment that the body won't reject like other highly toxic standard-of-care treatments.

Competing Receptors in TCR Therapy

In designing these engineered immune cell lines, problems are inevitably encountered, particularly in relation to competition with other immune cells or their

counterparts. For example, in the study preceding this one, antigen-specific TCRs were cloned into a mammalian expression vector and transfected via electroporation into a CD4+ Jurkat T cell line. The problem was: in evaluating whether these TCRs were functional, it was speculated that the endogenous TCRs competed with the synthetic, cloned TCRs for accessory proteins and space, potentially hybridizing with the receptor itself. Because the TCR is composed of two chains that assemble independently, there is a chance that there will be mismatches in the pairing of the two chains [73].

To mediate this, other studies have cloned TCRs into non-T cells, like HEK293 human kidney derivative cells [74]. Though in doing so, research has shown that synthetic TCRs can assemble at the membrane of these cells, functionality can not be determined because they lack the complex network of signals and accessory proteins responsible for TCR assembly, activation, and downstream cytokine release [75]. A naturally occurring, functional TCR is accompanied by CD3 molecules, the CD8 costimulatory protein, and ITAMs [76]. The CD3 dimers stabilize the TCR as it is formed and transported to the cell membrane for assembly, while the CD8 costimulatory protein binds to the MHC I molecule, stabilizing the immunologic synapse [77,78]. More specifically, the α chain interacts with the CD3d:CD3e dimer and a ζ dimer while the β chain interacts with one CD3g: CD3e dimer [79]. The charge between these subunits stabilizes the TCR complex and are responsible for intracellular signaling [77]. Each CD3 subunit has two immunoreceptor tyrosine-based activation motifs (ITAMS), and each ζ chain has three, equaling 10 ITAMs per TCR complex [76]. When their tyrosine residues are phosphorylated upon TCR binding to a ligand, a signaling cascade is initiated. In addition to increasing affinity at the immunological synapse, CD4 and CD8

coreceptors' intracellular kinase Lck is thought to be responsible for the tyrosine phosphorylation [80]. ZAP-70 then binds to the phosphorylated ITAMs, becoming phosphorylated itself [81]. This cascade of phosphorylation continues, ending with the release of transcription factors NFkB, NFAT, and AP-2, which control cell proliferation and differentiation [82]. Without these accessory proteins, there is the chance that the functionality of the TCR will be stifled or unable to bind to the MHC molecule presenting the antigen to stimulate a cytotoxic response. Because there is extensive internal and external machinery necessary for TCR assembly and activation, only a T cell line would suffice for cloning TCRs. However, there is no immortalized CD8⁺ T cell line on the market, so for the purposes of engineering a CD8⁺ cytotoxic T cell line, the CD8 coreceptor has to be integrated into a cell line as well.

Studies have been released attempting to immortalize CD8⁺ T cells, but none have been made readily available. One study attempted to immortalize CD8⁺ T cell clones by inducing the ectopic expression of the human telomerase reverse transcriptase (hTERT), but the study indicated prominent limitations [83]. Others have attempted to develop murine immortalized CD8⁺ T cell lines; however, these don't have the clinical applications of a human T cell line. As a result, pre-existing CD4⁺ T cell are the only vessel for hosting CD8⁺ TCRs.

TCR KSA Clone Transfection Characterization

To establish the same principle this knockout study was based off of, the results included the flow cytometry results from the transfection and tetramer staining of the KSA FluM1-specific TCR clone in nonA2 PBMCs (Fig. 3, 4). Because nonA2 donors

would be Flu-negative, positive results would indicate the presence of the construct at the membrane and its binding affinity. As seen in the figure, FluM1 tetramer did bind to the construct (Fig. 3). This figure illustrates the principle this study is working off of – only in the absence of endogenous receptors or the source of confounding variables could positive results be used to explain the presence of the synthetic TCR construct (Fig. 3). The other figure, indicating no binding affinity, serves as a visualization of what we expect to see in the absence of endogenous T cell receptors (Fig. 4). Ideally, there will be no binding to the Jurkat TCR antibodies post-transfection, as the CRISPR-Cas9 system should have knocked it out.

How to Combat Hybridization

To eliminate the potential for hybridization between synthetic and endogenous TCRs, we devised a pipeline for knocking out the naturally-occurring receptors with a CRISPR-Cas9 complex, targeting the constant region of the Jurkat TCR α and β constant region. gRNAs were designed to target sequences within the constant regions that confer low off-target potential but high binding affinity while occurring upstream of a Cas9-compatible PAM sequence. These gRNAs were delivered as phosphorylated, bound oligos with typeIIIs restriction sites for Golden Gate cloning into the CRISPR-compatible PX458 mammalian expression vector. The results indicated that the development of the delivery system, namely the RNP, was effective, with high levels of homology throughout the cloning process (Fig. 14, 15). As for the gRNAs, off-target potential was not tested due to shortened experiment time.

Guide RNAs and Off-Target Potential

The gRNAs, designed with the IDT Custom Alt-R CRISPR-Cas9 guide RNA design tool, yielded high off-target scores and on-target scores, indicating high specificity and binding affinity to the target gene, respectively (Fig. 7, 11). Though these values were >60 and fell within a region of the matrix where they were classified as effective, there was a significant margin of error, meaning there was still a chance the gRNAs could target the wrong genes or fail to bind to the target gene at all (Fig. 7, 11). This lack of specificity we see so often in designing gRNAs can be attributed to the small amount of homology needed for binding the Cas9 endonuclease and the wide range of Cas9-compatible PAM sequences present in a given genome [60]. Because the IDT Custom Alt-R CRISPR-Cas9 guide RNA design tool only looks at a given portion of the genome, its capabilities on predicting off-target potential for an entire cell's genome is limited; therefore, to evaluate this potential, other methods of design can be utilized where other portions of the genome are integrated into a predictive approach to reduce off-target potential (Fig. 8, 12).

Why Golden Gate Cloning

There were a plethora of studies that employed this same vector-based CRISPR-Cas9 complex delivery system [84]. In a one-pot process, a mix of ligase and restriction enzymes are added to a linearized vector and a purified product with complementary typeIIIs restriction sites [85]. Recombination of the product with the vector is mediated by a series of temperature changes. Golden Gate cloning is designed to minimize the introduction of extraneous sequences in the final product while providing researchers

with maximum control over the order and orientation of their sequences. Additionally, typeIIIs restriction sites are predetermined, and since the cloning method's inception, a wide array of GG-compatible vectors have been developed for a similarly wide range of purposes, eliminating the need for classic restriction enzyme cloning, which can require a high degree of customization [84]. One of the most attractive elements of Golden Gate cloning is the fact that the typeIIIs restriction sites are oriented in such a way that various sequences can be cloned and expressed in one vector [84]. The restriction enzymes cleave outside their recognition sequence, conserving the overhangs for assembly. Because each non-palindromic, four-base overhang is unique, their design specifies the order and orientation of the fragments, making the delivery of multiple sequences seamless [86]. This has been accomplished in lentiviral Golden Gate vectors, with as much as four sgRNAs being expressed in a single vector with one Cas9 endonuclease [87]. Eventually, as the pipeline for cloning and expressing gRNAs is optimized, co-expression of gRNAs for α and β chains could be entertained as a way to minimize reagent use and ensure that both chains are knocked out in a single transfection. Golden Gate is quickly becoming the standard for cloning, particularly in delivering CRISPR-Cas9 complexes. This is due to the fact that the materials needed to accomplish this are readily available and because so many researchers are familiar with the vector-based cloning protocols from other projects. However, the efficiency of Golden Gate post-transfection was not evaluated. If needs be, other cloning methods could be entertained such as Gateway or traditional restriction enzyme cloning, depending on reagent availability and cost.

In employing Golden Gate cloning, a high degree of homology was noted between intermediates of the protocol. The oligos containing the typeIIIs overhangs were

effectively phosphorylated and annealed, as illustrated by the EtBr gel (Fig. 13), and the one-pot protocol yielded a colony PCR with the predicted gRNA inserts (confirmed both by length and sequencing) (Fig. 14, 15).

Why the PX458 Vector

PX458, a mammalian expression vector supplied by the Feng Zhang lab, has various advantageous elements. The CRISPR-compatible vector contains a GFP tag for evaluating transfection efficiency, along with the Cas9 nuclease and scaffold, necessary to form the RNP within the cell. Encoding ampicillin resistance, the vector is compatible with the reagents most labs have. As a testament to this, the vector has been utilized in prior CRISPR-Cas9 studies accomplishing similar goals [88]. The BbsI sites were designed specifically to include short gRNA inserts, and they were placed so that the universal U6 promoter (LKO.1 5') primer could be used for downstream amplification or sequencing, reducing the need for customized primers. Achieving a high transfection efficiency through electroporating mammalian expression vectors is not a guarantee, as low transfection efficiency has been noted in past studies [89]. As a result, lentiviral vectors have been entertained as highly transfectable alternatives if PX458 does not yield results, namely pLX304, a Gateway-compatible, CRISPR-compatible vector [90].

What's the Best RNP Delivery Method

At the present time, transfection is a highly validated protocol. However, electroporation is considered to be highly toxic to cells and can yield a low transfection efficiency [89]. To mediate this and to find methods of delivering RNPs directly and

more rapidly, researchers are developing alternative protocols. That being said, these methods are early in development and costly to perform without having the right technology. Microinjections are one form of delivering RNPs *in vitro* or *ex vivo*, performed by injecting nucleic acids containing the gRNA and Cas9 enzyme directly into the cell cytoplasm or nucleus under a microscope [87]. Widely applicable adeno-associated virus (AAV) delivery utilizes viral particles to deliver CRISPR complexes into a cell *ex vivo* or *in vivo* [91]. These particles rarely trigger the human immune system as the virus isn't known to infect humans [91]. Similarly, lentiviruses and adenoviruses are utilized to deliver RNPs – they are roughly the same as AAV particles besides being larger in size [87]. In evaluating non-viral delivery methods, a multitude of studies have come out. Nucleic acids including Cas9 and the gRNA can also be delivered within lipid nanoparticles or cationic liposomes, which passively cross the membrane [92]. However, the cargo has to exit the endosome that forms within the cytoplasm before inducing any cell editing [87]. Other more recent forms of RNP delivery include lipoplexes, cell-penetrating peptides, the DNA nanoclew, and gold nanoparticles [87]. All of these nanoparticle delivery methods utilize the same principle of delivering the CRISPR complex directly into the cell without a cumbersome viral or bacterial vector. As a quickly evolving field, the world of CRISPR-Cas9 gene editing will see a multitude of new delivery methods, and as time passes, it will get easier to perform CRISPR-Cas9 gene editing with greater efficiency. This uptick in the number of delivery methods also provides researchers with more flexibility in designing experiments based on cost, accessibility, and the specific end goal of the study. For this study, the streamlined

transfection protocol and available technology made transfection of a mammalian expression vector the best fit.

What Makes CRISPR the Best Gene Editing Protocol

Not only are there various delivery methods within CRISPR-Cas9 tech, but there are also a multitude of gene editing methods that have yet to be explored for the purposes of this study. All three of the widely used gene editing technologies, zinc finger nucleases, TALENs, and CRISPR, have been utilized to knock out TCR sequences in past studies, opening up more avenues for this course of work [93, 94]. In one study, ZFNs were utilized to knock out HLA molecules and host TCRs to prevent self-reactivity in CD19+ malignancies [93]. In another study, both TALENs and gRNAs (as part of a CRISPR-Cas9 complex) were designed to knock out endogenous TCRs [94]. Surprisingly, both the TALENs and the gRNAs yielded >80% efficiency with low off-target effects [94]. Although there were successes in these studies, they are few and far between, due to CRISPR-Cas9 being the new gold standard of gene editing. Although TALENs have been around for longer, CRISPR-Cas9 has jumped to the forefront of gene editing due to its significantly lower cost [95]. In a comparative study, it was found that CRISPR gene editing was up to 10 times cheaper for all forms of gene editing (gene knockout or knock-in, gene silencing, and gene upregulation or downregulation) [95]. Other studies cite that it's more accurate and programmable. However, there are some drawbacks, such as the limitation of choosing sequences that fall upstream of a PAM sequence and the large Cas9 nuclease, which is challenging to deliver into cells [96]. That being said, the fact that Cas9 has predetermined signal sequences reduces the need for a

customized nuclease, furthering the flexibility of the gene editing technique. For this knockout experiment, the simplicity in designing targets as well as the low cost make it the optimal candidate.

Gene Editing Accuracy

CRISPR, despite being the gold standard for gene editing, doesn't offer the guarantee that the right gene will be manipulated, nor does it offer the guarantee that the target gene alone will be manipulated. CRISPR is a feasible option for knocking in or knocking a gene out, but characterizing whether the complex was effective in doing so is lengthy, and there may be unknown downstream consequences that are not initially observable. The off-target effects observed in CRISPR-Cas9 have been widely studied due to health concerns for *in vivo* gene editing and in hopes of optimizing the gene editing technique for *ex vivo* purposes [65]. During sequence recognition, where the seed sequence binds to the region adjacent to the PAM, it was found that as much as three to five base pair mismatches in the ~20 nt sequence permitted enough homology to bind and induce a double-stranded break [65]. The study, which compiled findings from other research concluded that the off-target activity of RNA guided endonucleases was >50% [65]. Methods have been devised to mediate this inaccuracy, however.

Utilizing Cas9 nickase, a D10A mutant of SpCas9, where a nick is generated in lieu of a double-stranded break, increases specificity because two nicks on complementary DNA strands are required to induce a double-stranded break – creating two off-target nicks (to constitute a DSB) in the same location is unlikely [97]. Cytosine base editors (CBEs) and adenine base editors (ABEs) are other methods devised to

overcome the inaccuracies of CRISPR-Cas9. By fusing a Cas9 nickase or a deactivated Cas9 (dCas9) nuclease to a nucleobase deaminase enzyme, specific loci can be targeted via gRNAs, where cytidine is converted to uridine upon recognition of the PAM site [98]. These variations of the CRISPR-Cas9 complex allow for greater accuracy in gene editing, and although it's virtually impossible to eliminate the off-target effects of a CRISPR complex, as research proceeds, these effects will continue to be minimized.

Developing a Functional CD8⁺ T Cell Line

Though the results indicate that this project is suited for CRISPR-Cas9 gene editing, there is the question of whether the end goal of generating a CD8⁺ T cell line is possible. Because no immortalized CD8⁺ T cell line exists, researchers have to work with CD4⁺ T cell lines, adding whatever components they need for the immunotherapy they are pursuing. In theory, this should work – knocking out CD4 coreceptors and adding CD8⁺ TCRs should confer a cytotoxic response. However, there is limited information on whether CD4⁺ helper T cells can be wholly converted to CD8⁺ cytotoxic T cells. The signaling pathways between CD4⁺ and CD8⁺ T cells are largely the same with studies identifying CD4⁺ cytotoxic T cells *in vivo* [99]. This suggests that they possess perforin and granzyme particles for use in cytotoxic responses. However, more research needs to be done to establish what conditions are needed for the expression of this phenotype. Current characterization techniques for measuring activation and functionality of the synthetic CD8⁺ TCRs in Jurkats are currently limited to measuring cytokine release such as IL-2 [100]. Jurkats are customarily limited to the release of cytokine IL-2 and the release of chemokines MCP-1, MIP-1 β , IL-8, and MIP-1 α [100]. However, in time,

cytotoxicity assays may be usable to determine whether Jurkats are not only activated, but also whether they have cell-killing capabilities.

Other Applications of CRISPR

Such an experiment is a testament to the validity of CRISPR-Cas9 gene editing in practice, but CRISPR gene editing has potential far beyond knocking out immune receptors. CRISPR germline gene editing could be used to knock out genes coding for susceptibility to infectious diseases or congenital disorders. This concept has been met with a high degree of controversy, and only *ex vivo* CRISPR gene editing has been mandated as legal or “safe” [103]. Germline gene editing and embryonic gene editing can alter the expression of inheritable genes and the phenotypes they code for. For example, CCR5 encodes susceptibility to cholera, smallpox, and HIV while certain HLA subtypes confer higher risk or protection to autoimmune disorders and infection [100,101]. Altering these genes to be upregulated or downregulated via CRISPR could confer a health advantage; however, this form of genomic alteration is far off due to ethical implications and research restrictions.

A Broadly Applicable KO T Cell Line

The study, in evaluating methods of harnessing CRISPR-Cas9’s abilities to knock out a given gene, addresses the need for a broadly applicable CD8+ KO TCR T cell line in developing immunotherapies. These immunotherapies are not confined to treating cancer alone, nor do the immune receptors cloned in need to be naturally-occurring TCRs. For any construct expressed on the cell surface, there would no longer be competition for

space, proliferative signaling, or stabilization from accessory proteins. Developing this cell line served not only as a way to create a vessel for the antigen-specific TCR constructs developed for this lab's T cell immunotherapy project, but it also provides a reproducible protocol for engineering future CD4+ T cell lines to accomplish the same goal for future projects.

REFERENCES

1. Nagai H, Kim YH. Cancer prevention from the perspective of global cancer burden patterns. *Journal of thoracic disease*. 2017. pp. 448–451.
2. Hanahan D, Weinberg RA. Hallmarks of cancer: the next generation. *Cell*. 2011;144: 646–674.
3. West J, You L, Zhang J, Gatenby RA, Brown JS, Newton PK, et al. Towards Multidrug Adaptive Therapy. *Cancer Res*. 2020;80: 1578–1589.
4. Etzioni R, Gulati R, Lin DW. Measures of survival benefit in cancer drug development and their limitations. *Urol Oncol*. 2015;33: 122–127.
5. Arruebo M, Vilaboa N, Sáez-Gutierrez B, Lambea J, Tres A, Valladares M, et al. Assessment of the evolution of cancer treatment therapies. *Cancers* . 2011;3: 3279–3330.
6. Rosenberg SA, Restifo NP, Yang JC, Morgan RA, Dudley ME. Adoptive cell transfer: a clinical path to effective cancer immunotherapy. *Nat Rev Cancer*. 2008;8: 299–308.
7. Lee S, Margolin K. Tumor-infiltrating lymphocytes in melanoma. *Curr Oncol Rep*. 2012;14: 468–474.
8. Miliotou AN, Papadopoulou LC. CAR T-cell Therapy: A New Era in Cancer Immunotherapy. *Curr Pharm Biotechnol*. 2018;19: 5–18.
9. Ping Y, Liu C, Zhang Y. T-cell receptor-engineered T cells for cancer treatment: current status and future directions. *Protein Cell*. 2018;9: 254–266.
10. Kosaka Y, Keating A. Natural Killer Cells for Cancer Immunotherapy. *Experimental and Applied Immunotherapy*. 2011. pp. 85–105. doi:10.1007/978-1-60761-980-2_4
11. Zhang J, Wang L. The Emerging World of TCR-T Cell Trials Against Cancer: A Systematic Review. *Technol Cancer Res Treat*. 2019;18: 1533033819831068.
12. Nagoshi M, Sadanaga N, Joo H-G, Goedegebuure PS, Eberlein TJ. Tumor-specific cytokine release by donor T cells induces an effective host anti-tumor response through recruitment of host naive antigen presenting cells. *International journal of cancer*. 1999;80: 308–314.
13. Cope AP. Studies of T-cell activation in chronic inflammation. *Arthritis Res*. 2002;4 Suppl 3: S197–211.
14. Inoue M, Shinohara ML. Hyperinflammation, T cells, and endotoxemia. *Oncotarget*. 2015. pp. 23040–23041.

15. Laydon DJ, Bangham CRM, Asquith B. Estimating T-cell repertoire diversity: limitations of classical estimators and a new approach. *Philosophical Transactions of the Royal Society B: Biological Sciences*. 2015. p. 20140291. doi:10.1098/rstb.2014.0291
16. Lythe G, Callard RE, Hoare RL, Molina-París C. How many TCR clonotypes does a body maintain? *J Theor Biol*. 2016;389: 214–224.
17. Chien YH, Gascoigne NR, Kavaler J, Lee NE, Davis MM. Somatic recombination in a murine T-cell receptor gene. *Nature*. 1984;309: 322–326.
18. Ma L, Yang L, Shi B, He X, Peng A, Li Y, et al. Analyzing the CDR3 Repertoire with respect to TCR—Beta Chain VDJ and VJ Rearrangements in Peripheral T Cells using HTS. *Sci Rep*. 2016;6: 1–10.
19. Klarenbeek PL, Doorenspleet ME, Esveldt REE, van Schaik BDC, Lardy N, van Kampen AHC, et al. Somatic Variation of T-Cell Receptor Genes Strongly Associate with HLA Class Restriction. *PLoS One*. 2015;10: e0140815.
20. Uttenthal BJ, Chua I, Morris EC, Stauss HJ. Challenges in T cell receptor gene therapy. *J Gene Med*. 2012;14: 386–399.
21. Saito T, Hochstenbach F, Marusic-Galesic S, Kruisbeek AM, Brenner M, Germain RN. Surface expression of only gamma delta and/or alpha beta T cell receptor heterodimers by cells with four (alpha, beta, gamma, delta) functional receptor chains. *The Journal of Experimental Medicine*. 1988. pp. 1003–1020. doi:10.1084/jem.168.3.1003
22. Zhao Y, Niu C, Cui J. Gamma-delta ($\gamma\delta$) T cells: friend or foe in cancer development? *J Transl Med*. 2018;16: 3.
23. Nussbaumer O, Koslowski M. The emerging role of $\gamma\delta$ T cells in cancer immunotherapy. *Immuno-Oncology Technology*. 2019. pp. 3–10. doi:10.1016/j.iotech.2019.06.002
24. Luckheeram RV, Zhou R, Verma AD, Xia B. CD4 T Cells: Differentiation and Functions. *Clinical and Developmental Immunology*. 2012. pp. 1–12. doi:10.1155/2012/925135
25. Osińska I, Popko K, Demkow U. Perforin: an important player in immune response. *Cent Eur J Immunol*. 2014;39: 109–115.
26. Roberts CA, Dickinson AK, Taams LS. The Interplay Between Monocytes/Macrophages and CD4 T Cell Subsets in Rheumatoid Arthritis. *Frontiers in Immunology*. 2015. doi:10.3389/fimmu.2015.00571
27. Farber DL, Yudanin NA, Restifo NP. Human memory T cells: generation, compartmentalization and homeostasis. *Nat Rev Immunol*. 2014;14: 24–35.

28. Murali-Krishna K, Altman JD, Suresh M, Sourdive DJ, Zajac AJ, Miller JD, et al. Counting antigen-specific CD8 T cells: a reevaluation of bystander activation during viral infection. *Immunity*. 1998;8: 177–187.
29. Wang J-H, Reinherz EL. The structural basis of $\alpha\beta$ T-lineage immune recognition: TCR docking topologies, mechanotransduction, and co-receptor function. *Immunological Reviews*. 2012. pp. 102–119. doi:10.1111/j.1600-065x.2012.01161.x
30. Shao H, Zhang W, Hu Q, Wu F, Shen H, Huang S. TCR mispairing in genetically modified T cells was detected by fluorescence resonance energy transfer. *Mol Biol Rep*. 2010;37: 3951–3956.
31. Simone MD, De Simone M, Rossetti G, Pagani M. Single Cell T Cell Receptor Sequencing: Techniques and Future Challenges. *Frontiers in Immunology*. 2018. doi:10.3389/fimmu.2018.01638
32. Reece-Hoyes JS, Walhout AJM. Gateway Recombinational Cloning. *Cold Spring Harb Protoc*. 2018;2018. doi:10.1101/pdb.top094912
33. Dobson-Belaire WN, Cochrane A, Ostrowski MA, Gray-Owen SD. Differential Response of Primary and Immortalized CD4 T Cells to *Neisseria gonorrhoeae*-Induced Cytokines Determines the Effect on HIV-1 Replication. *PLoS ONE*. 2011. p. e18133. doi:10.1371/journal.pone.0018133
34. Live and Let Live: The Remarkable Story of HEK293 Cells. *Hum Gene Ther*. 2020;31: 485–487.
35. Chandran SS, Klebanoff CA. T cell receptor-based cancer immunotherapy: Emerging efficacy and pathways of resistance. *Immunol Rev*. 2019;290: 127–147.
36. Walseng E, Köksal H, Sektioglu IM, Fåne A, Skorstad G, Kvalheim G, et al. A TCR-based Chimeric Antigen Receptor. *Sci Rep*. 2017;7: 10713.
37. Bethune MT, Gee MH, Bunse M, Lee MS, Gschweng EH, Pagadala MS, et al. Domain-swapped T cell receptors improve the safety of TCR gene therapy. *eLife*. 2016. doi:10.7554/elife.19095
38. Bunse M, Bendle GM, Linnemann C, Bies L, Schulz S, Schumacher TN, et al. RNAi-mediated TCR Knockdown Prevents Autoimmunity in Mice Caused by Mixed TCR Dimers Following TCR Gene Transfer. *Molecular Therapy*. 2014. pp. 1983–1991. doi:10.1038/mt.2014.142
39. Legut M, Dolton G, Mian AA, Ottmann OG, Sewell AK. CRISPR-mediated TCR replacement generates superior anticancer transgenic T cells. *Blood*. 2018;131: 311–322.

40. Cole DK, Laugel B, Clement M, Price DA, Wooldridge L, Sewell AK. The molecular determinants of CD8 co-receptor function. *Immunology*. 2012. pp. 139–148. doi:10.1111/j.1365-2567.2012.03625.x
41. Koretzky GA. Multiple Roles of CD4 and CD8 in T Cell Activation. *The Journal of Immunology*. 2010. pp. 2643–2644. doi:10.4049/jimmunol.1090076
42. Haggerty TJ, Dunn IS, Rose LB, Newton EE, Kurnick JT. A Screening Assay to Identify Agents That Enhance T-Cell Recognition of Human Melanomas. *ASSAY and Drug Development Technologies*. 2012. pp. 187–201. doi:10.1089/adt.2011.0379
43. Carroll D. Genome Engineering With Zinc-Finger Nucleases. *Genetics*. 2011. pp. 773–782. doi:10.1534/genetics.111.131433
44. Do TU, Ho B, Shih S-J, Vaughan A. Zinc Finger Nuclease induced DNA double stranded breaks and rearrangements in MLL. *Mutation Research/Fundamental and Molecular Mechanisms of Mutagenesis*. 2012. pp. 34–42. doi:10.1016/j.mrfmmm.2012.12.006
45. Nambiar TS, Billon P, Diedenhofen G, Hayward SB, Taglialatela A, Cai K, et al. Stimulation of CRISPR-mediated homology-directed repair by an engineered RAD18 variant. *Nat Commun*. 2019;10: 3395.
46. Joung JK, Keith Joung J, Sander JD. TALENs: a widely applicable technology for targeted genome editing. *Nature Reviews Molecular Cell Biology*. 2013. pp. 49–55. doi:10.1038/nrm3486
47. Hsu PD, Lander ES, Zhang F. Development and Applications of CRISPR-Cas9 for Genome Engineering. *Cell*. 2014. pp. 1262–1278. doi:10.1016/j.cell.2014.05.010
48. Wilbie D, Walther J, Mastrobattista E. Delivery Aspects of CRISPR/Cas for in Vivo Genome Editing. *Accounts of Chemical Research*. 2019. pp. 1555–1564. doi:10.1021/acs.accounts.9b00106
49. Ishino Y, Krupovic M, Forterre P. History of CRISPR-Cas from Encounter with a Mysterious Repeated Sequence to Genome Editing Technology. *Journal of Bacteriology*. 2018. doi:10.1128/jb.00580-17
50. Barrangou R, Marraffini LA. CRISPR-Cas Systems: Prokaryotes Upgrade to Adaptive Immunity. *Molecular Cell*. 2014. pp. 234–244. doi:10.1016/j.molcel.2014.03.011
51. Loureiro A, da Silva G. CRISPR-Cas: Converting A Bacterial Defence Mechanism into A State-of-the-Art Genetic Manipulation Tool. *Antibiotics*. 2019. p. 18. doi:10.3390/antibiotics8010018

52. Greely HT. CRISPR'd babies: human germline genome editing in the "He Jiankui affair"*. *Journal of Law and the Biosciences*. 2019. pp. 111–183. doi:10.1093/jlb/lbz010
53. Wang H, Yang H. Gene-edited babies: What went wrong and what could go wrong. *PLoS Biol*. 2019;17: e3000224.
54. Li J-R, Walker S, Nie J-B, Zhang X-Q. Experiments that led to the first gene-edited babies: the ethical failings and the urgent need for better governance. *Journal of Zhejiang University-SCIENCE B*. 2019. pp. 32–38. doi:10.1631/jzus.b1800624
55. Liu M, Rehman S, Tang X, Gu K, Fan Q, Chen D, et al. Methodologies for Improving HDR Efficiency. *Front Genet*. 2018;9: 691.
56. Guo T, Feng Y-L, Xiao J-J, Liu Q, Sun X-N, Xiang J-F, et al. Harnessing accurate non-homologous end joining for efficient precise deletion in CRISPR/Cas9-mediated genome editing. *Genome Biol*. 2018;19: 170.
57. Zhang J-P, Li X-L, Li G-H, Chen W, Arakaki C, Botimer GD, et al. Efficient precise knockin with a double cut HDR donor after CRISPR/Cas9-mediated double-stranded DNA cleavage. *Genome Biol*. 2017;18: 35.
58. Adli M. The CRISPR tool kit for genome editing and beyond. *Nature Communications*. 2018. doi:10.1038/s41467-018-04252-2
59. Ratan ZA, Son Y-J, Haidere MF, Uddin BMM, Yusuf MA, Zaman SB, et al. CRISPR-Cas9: a promising genetic engineering approach in cancer research. *Ther Adv Med Oncol*. 2018;10: 1758834018755089.
60. Gleditsch D, Pausch P, Müller-Esparza H, Özcan A, Guo X, Bange G, et al. PAM identification by CRISPR-Cas effector complexes: diversified mechanisms and structures. *RNA Biology*. 2019. pp. 504–517. doi:10.1080/15476286.2018.1504546
61. Liu C, Zhang L, Liu H, Cheng K. Delivery strategies of the CRISPR-Cas9 gene-editing system for therapeutic applications. *J Control Release*. 2017;266: 17–26.
62. DeWitt MA, Corn JE, Carroll D. Genome editing via delivery of Cas9 ribonucleoprotein. *Methods*. 2017. pp. 9–15. doi:10.1016/j.ymeth.2017.04.003
63. Rouet R, Thuma BA, Roy MD, Lintner NG, Rubitski DM, Finley JE, et al. Receptor-Mediated Delivery of CRISPR-Cas9 Endonuclease for Cell-Type-Specific Gene Editing. *J Am Chem Soc*. 2018;140: 6596–6603.
64. Fu Y, Foden JA, Khayter C, Maeder ML, Reyon D, Joung JK, et al. High-frequency off-target mutagenesis induced by CRISPR-Cas nucleases in human cells. *Nat Biotechnol*. 2013;31: 822–826.

65. Zhang X-H, Tee LY, Wang X-G, Huang Q-S, Yang S-H. Off-target Effects in CRISPR/Cas9-mediated Genome Engineering. *Mol Ther Nucleic Acids*. 2015;4: e264.
66. Hastings KG, Kapphahn K, Boothroyd DB, Rehkopf DH, Cullen MR, Palaniappan L. Transition From Heart Disease to Cancer as the Leading Cause of Death in the United States. *Annals of internal medicine*. 2019. p. 225.
67. Dudley ME, Rosenberg SA. Adoptive-cell-transfer therapy for the treatment of patients with cancer. *Nature Reviews Cancer*. 2003. pp. 666–675. doi:10.1038/nrc1167
68. Houot R, Schultz LM, Marabelle A, Kohrt H. T-cell-based Immunotherapy: Adoptive Cell Transfer and Checkpoint Inhibition. *Cancer Immunol Res*. 2015;3: 1115–1122.
69. Kataoka T. Adaptive and Innate Immune Systems. *Bioprobes*. 2017. pp. 115–147. doi:10.1007/978-4-431-56529-1_5
70. Janeway CA Jr, Medzhitov R. Innate immune recognition. *Annu Rev Immunol*. 2002;20: 197–216.
71. Pennock ND, White JT, Cross EW, Cheney EE, Tamburini BA, Kedl RM. T cell responses: naïve to memory and everything in between. *Advances in Physiology Education*. 2013. pp. 273–283. doi:10.1152/advan.00066.2013
72. Goulder PJR, Walker BD. HIV and HLA Class I: An Evolving Relationship. *Immunity*. 2012. pp. 426–440. doi:10.1016/j.immuni.2012.09.005
73. Bialer G, Horovitz-Fried M, Ya'acobi S, Morgan RA, Cohen CJ. Selected Murine Residues Endow Human TCR with Enhanced Tumor Recognition. *The Journal of Immunology*. 2010. pp. 6232–6241. doi:10.4049/jimmunol.0902047
74. Walseng E, Wälchli S, Fallang L-E, Yang W, Vefferstad A, Areffard A, et al. Soluble T-cell receptors produced in human cells for targeted delivery. *PLoS One*. 2015;10: e0119559.
75. Sharpe M, Mount N. Genetically modified T cells in cancer therapy: opportunities and challenges. *Dis Model Mech*. 2015;8: 337–350.
76. Love PE, Hayes SM. ITAM-mediated Signaling by the T-Cell Antigen Receptor. *Cold Spring Harbor Perspectives in Biology*. 2010. pp. a002485–a002485. doi:10.1101/cshperspect.a002485
77. Call ME, Wucherpennig KW. Molecular mechanisms for the assembly of the T cell receptor–CD3 complex. *Molecular Immunology*. 2004. pp. 1295–1305. doi:10.1016/j.molimm.2003.11.017

78. Varghese JC, Kane KP. TCR Complex-Activated CD8 Adhesion Function by Human T Cells. *The Journal of Immunology*. 2008. pp. 6002–6009. doi:10.4049/jimmunol.181.9.6002
79. Davignon J-L, Arnold LW, Cohen PL, Eisenberg RA. CD3 expression, modulation and signalling in T-cell subpopulations from MRLMp-lprlpr mice. *J Autoimmun*. 1991;4: 831–844.
80. Rossy J, Williamson DJ, Gaus K. How does the kinase Lck phosphorylate the T cell receptor? Spatial organization as a regulatory mechanism. *Frontiers in Immunology*. 2012. doi:10.3389/fimmu.2012.00167
81. Wang H, Kadlec TA, Au-Yeung BB, Goodfellow HES, Hsu LY, Freedman TS, et al. ZAP-70: An Essential Kinase in T-cell Signaling. *Cold Spring Harbor Perspectives in Biology*. 2010. pp. a002279–a002279. doi:10.1101/cshperspect.a002279
82. Watanabe N. Regulation of NFkB1 proteins by the candidate oncoprotein BCL-3: generation of NF-kappa B homodimers from the cytoplasmic pool of p50-p105 and nuclear translocation. *The EMBO Journal*. 1997. pp. 3609–3620. doi:10.1093/emboj/16.12.3609
83. Hooijberg E, Ruizendaal JJ, Snijders PJF, Kueter EWM, Walboomers JMM, Spits H. Immortalization of Human CD8 T Cell Clones by Ectopic Expression of Telomerase Reverse Transcriptase. *The Journal of Immunology*. 2000. pp. 4239–4245. doi:10.4049/jimmunol.165.8.4239
84. Liu X, Zhou X, Li K, Wang D, Ding Y, Liu X, et al. A simple and efficient cloning system for CRISPR/Cas9-mediated genome editing in rice. *PeerJ*. 2020;8: e8491.
85. Engler C, Marillonnet S. Combinatorial DNA Assembly Using Golden Gate Cloning. *Synthetic Biology*. 2013. pp. 141–156. doi:10.1007/978-1-62703-625-2_12
86. Chiasson D, Giménez-Oya V, Bircheneder M, Bachmaier S, Studtrucker T, Ryan J, et al. A unified multi-kingdom Golden Gate cloning platform. *Scientific Reports*. 2019. doi:10.1038/s41598-019-46171-2
87. Lino CA, Harper JC, Carney JP, Timlin JA. Delivering CRISPR: a review of the challenges and approaches. *Drug Delivery*. 2018. pp. 1234–1257. doi:10.1080/10717544.2018.1474964
88. Cong L, Zhang F. Genome Engineering Using CRISPR-Cas9 System. *Chromosomal Mutagenesis*. 2015. pp. 197–217. doi:10.1007/978-1-4939-1862-1_10
89. Seki A, Rutz S. Optimized RNP transfection for highly efficient CRISPR/Cas9-mediated gene knockout in primary T cells. *J Exp Med*. 2018;215: 985–997.

90. Yang X, Boehm JS, Yang X, Salehi-Ashtiani K, Hao T, Shen Y, et al. A public genome-scale lentiviral expression library of human ORFs. *Nature Methods*. 2011. pp. 659–661. doi:10.1038/nmeth.1638
91. Mueller C, Flotte TR. Clinical gene therapy using recombinant adeno-associated virus vectors. *Gene Therapy*. 2008. pp. 858–863. doi:10.1038/gt.2008.68
92. Zuris JA, Thompson DB, Shu Y, Guilinger JP, Bessen JL, Hu JH, et al. Cationic lipid-mediated delivery of proteins enables efficient protein-based genome editing in vitro and in vivo. *Nat Biotechnol*. 2015;33: 73–80.
93. Torikai H, Reik A, Yuen C, Zhou Y, Kellar D, Huls H, et al. HLA and TCR Knockout by Zinc Finger Nucleases: Toward “off-the-Shelf” Allogeneic T-Cell Therapy for CD19 Malignancies. *Blood*. 2010. pp. 3766–3766. doi:10.1182/blood.v116.21.3766.3766
94. Knipping F, Osborn MJ, Petri K, Tolar J, Glimm H, von Kalle C, et al. Genome-wide Specificity of Highly Efficient TALENs and CRISPR/Cas9 for T Cell Receptor Modification. *Molecular Therapy - Methods & Clinical Development*. 2017. pp. 213–224. doi:10.1016/j.omtm.2017.01.005
95. Bhattacharya D, Marfo CA, Li D, Lane M, Khokha MK. CRISPR/Cas9: An inexpensive, efficient loss of function tool to screen human disease genes in *Xenopus*. *Developmental Biology*. 2015. pp. 196–204. doi:10.1016/j.ydbio.2015.11.003
96. Li L, He Z-Y, Wei X-W, Gao G-P, Wei Y-Q. Challenges in CRISPR/CAS9 Delivery: Potential Roles of Nonviral Vectors. *Hum Gene Ther*. 2015;26: 452–462.
97. Cho SW, Kim S, Kim Y, Kweon J, Kim HS, Bae S, et al. Analysis of off-target effects of CRISPR/Cas-derived RNA-guided endonucleases and nickases. *Genome Research*. 2014. pp. 132–141. doi:10.1101/gr.162339.113
98. Rees HA, Liu DR. Base editing: precision chemistry on the genome and transcriptome of living cells. *Nat Rev Genet*. 2018;19: 770–788.
99. Takeuchi A, Saito T. CD4 CTL, a Cytotoxic Subset of CD4+ T Cells, Their Differentiation and Function. *Front Immunol*. 2017;8: 194.
100. Bartelt RR, Cruz-Orcutt N, Collins M, Houtman JCD. Comparison of T cell receptor-induced proximal signaling and downstream functions in immortalized and primary T cells. *PLoS One*. 2009;4: e5430.
101. Barmania F, Pepper MS. C-C chemokine receptor type five (CCR5): An emerging target for the control of HIV infection. *Appl Transl Genom*. 2013;2: 3–16.
102. Blackwell JM, Jamieson SE, Burgner D. HLA and infectious diseases. *Clin Microbiol Rev*. 2009;22: 370–85, Table of Contents.

103. Grant EV. FDA Regulation of Clinical Applications of CRISPR-CAS Gene-Editing Technology. Food Drug Law J. 2016;71: 608–633.
104. Idtdna.com, www.idtdna.com/site/order/designtool/index/CRISPR_CUSTOM.

APPENDIX A
SUPPLEMENTARY TABLES

Supplementary Table 1: Guide RNA designs targeting α constant region of the Jurkat TCR sequence. This includes both the sense and antisense strand with the accompanying Golden Gate typeIIIs restriction sites (bolded) as well as the 5' end guanine base (in parentheses). The U6 promoter requires the first nucleotide of the insert to be guanine.

gRNA	Sequence
gRNA α No. 1 sense 5'-3'	CACC(G) AAGTTCCTGTGATGTCAAGC
gRNA α No. 1 antisense 5'-3'	AAACGCTT GACATCACAGGAACTT
gRNA α No. 2 sense 5'-3'	CACC(G) TTCGGAACCCAATCACTGAC
gRNA α No. 2 antisense 5'-3'	AAACGTCAGT GATTGGGTTCGGAAC

Supplementary Table 2: Guide RNA designs targeting β constant region of the Jurkat TCR sequence. This includes both the sense and antisense strand with the accompanying Golden Gate typeIIIs restriction sites (bolded) as well as the 5' end guanine base (in parentheses). The U6 promoter requires the first nucleotide of the insert to be guanine.

gRNA	Sequence
gRNA β No. 1 sense 5'-3'	CACC(G) AGGCTTCTACCCCGACCACG
gRNA β No. 1 antisense 5'-3'	AAACCGTGGT CGGGGTAGAAGCCTC
gRNA β No. 2 sense 5'-3'	CACC(G) GACCAGCACGGCATAACAAGG
gRNA β No. 2 antisense 5'-3'	AAACCCTTGT ATGCCGTGCTGGTCC

Supplementary Table 3: Reverse primer designs for guide RNA amplification and sequencing. The reverse primers (CS1 and CS2) were customized to fall just outside the second BbSI restriction site, as to encompass and amplify the entire gRNA insert ligated into the PX458 vector.

gRNA	Sequence	Tm (Celsius)	Length (bp)
PX458 Rev (CS1)	TCGGTGCCAACTTTTCA	51.9	19
PX458 Rev (CS2)	CGGACTAGCCTTAGC	48.4	15

Supplementary Table 4: One-step PCR protocol for gRNA amplification. DreamTaq HS polymerase was used (Thermo Fisher).

Temperature (Celsius)	Time	Cycles
95	3:00	Hold
95	0:30	30 cycles
48	0:30	30 cycles
72	1:00	30 cycles
72	5:00	Hold
4	Inf.	Hold